

This work was written as part of one of the author's official duties as an Employee of the United States Government and is therefore a work of the United States Government. In accordance with 17 U.S.C. 105, no copyright protection is available for such works under U.S. Law.

Public Domain Mark 1.0

<https://creativecommons.org/publicdomain/mark/1.0/>

Access to this work was provided by the University of Maryland, Baltimore County (UMBC) ScholarWorks@UMBC digital repository on the Maryland Shared Open Access (MD-SOAR) platform.

**Please provide feedback**

Please support the ScholarWorks@UMBC repository by emailing [scholarworks-group@umbc.edu](mailto:scholarworks-group@umbc.edu) and telling us what having access to this work means to you and why it's important to you. Thank you.

## RESEARCH ARTICLE

10.1002/2015JD024121

## Key Points:

- Notable changes in NO<sub>2</sub> levels globally and their causes over last decade
- High-resolution OMI NO<sub>2</sub> data show large spatial heterogeneity in world's megacities
- There is a strong need to develop observational networks in tropics and subtropics

## Supporting Information:

- Tables S1–S9 and Figures S1–S4

## Correspondence to:

B. N. Duncan,  
Bryan.N.Duncan@nasa.gov

## Citation:

Duncan, B. N., L. N. Lamsal, A. M. Thompson, Y. Yoshida, Z. Lu, D. G. Streets, M. M. Hurwitz, and K. E. Pickering (2016), A space-based, high-resolution view of notable changes in urban NO<sub>x</sub> pollution around the world (2005–2014), *J. Geophys. Res. Atmos.*, 121, 976–996, doi:10.1002/2015JD024121.

Received 21 AUG 2015

Accepted 15 DEC 2015

Accepted article online 18 DEC 2015

Published online 20 JAN 2016

A space-based, high-resolution view of notable changes in urban NO<sub>x</sub> pollution around the world (2005–2014)

Bryan N. Duncan<sup>1</sup>, Lok N. Lamsal<sup>1,2</sup>, Anne M. Thompson<sup>1</sup>, Yasuko Yoshida<sup>1,3</sup>, Zifeng Lu<sup>4</sup>, David G. Streets<sup>4</sup>, Margaret M. Hurwitz<sup>1,5</sup>, and Kenneth E. Pickering<sup>1</sup>
<sup>1</sup>NASA Goddard Space Flight Center, Greenbelt, Maryland, USA, <sup>2</sup>Goddard Earth Sciences Technology and Research, Universities Space Research Association, Columbia, Maryland, USA, <sup>3</sup>Science Systems and Applications, Inc., Greenbelt, Maryland, USA, <sup>4</sup>Argonne National Laboratory, Argonne, Illinois, USA, <sup>5</sup>GESTAR, Morgan State University, Baltimore, Maryland, USA

**Abstract** Nitrogen oxides (NO<sub>x</sub> = NO + NO<sub>2</sub>) are produced during combustion processes and, thus may serve as a proxy for fossil fuel-based energy usage and coemitted greenhouse gases and other pollutants. We use high-resolution nitrogen dioxide (NO<sub>2</sub>) data from the Ozone Monitoring Instrument (OMI) to analyze changes in urban NO<sub>2</sub> levels around the world from 2005 to 2014, finding complex heterogeneity in the changes. We discuss several potential factors that seem to determine these NO<sub>x</sub> changes. First, environmental regulations resulted in large decreases. The only large increases in the United States may be associated with three areas of intensive energy activity. Second, elevated NO<sub>2</sub> levels were observed over many Asian, tropical, and subtropical cities that experienced rapid economic growth. Two of the largest increases occurred over recently expanded petrochemical complexes in Jamnagar (India) and Daesan (Korea). Third, pollution transport from China possibly influenced the Republic of Korea and Japan, diminishing the impact of local pollution controls. However, in China, there were large decreases over Beijing, Shanghai, and the Pearl River Delta, which were likely associated with local emission control efforts. Fourth, civil unrest and its effect on energy usage may have resulted in lower NO<sub>2</sub> levels in Libya, Iraq, and Syria. Fifth, spatial heterogeneity within several megacities may reflect mixed efforts to cope with air quality degradation. We also show the potential of high-resolution data for identifying NO<sub>x</sub> emission sources in regions with a complex mix of sources. Intensive monitoring of the world's tropical/subtropical megacities will remain a priority, as their populations and emissions of pollutants and greenhouse gases are expected to increase significantly.

## 1. Introduction

A family of trace gases, nitrogen oxides (NO<sub>x</sub> = NO + NO<sub>2</sub>), is primarily emitted to the atmosphere during fossil fuel combustion. NO<sub>x</sub> emissions are regulated in many countries, as NO<sub>2</sub> is unhealthy to breathe, and NO<sub>x</sub> is a necessary ingredient for the formation of surface ozone, a pollutant that is not readily quantified near the surface with data from current space-based instruments [Fishman et al., 2008; Bowman, 2013]. A change in NO<sub>x</sub> levels can serve as a proxy for a change in (1) NO<sub>x</sub> emissions [e.g., Streets et al., 2013], (2) energy consumption using a characteristic emission intensity, such as the amount of NO<sub>x</sub> emitted per unit coal or gasoline combusted, and (3) emissions of coemitted gases, including pollutants and greenhouse gases that cannot be measured (or measured adequately) with current space-based technology. Inferences of changes in energy usage and coemitted gases from NO<sub>x</sub> levels require careful attention to factors, such as the type of coal combusted [e.g., Liu et al., 2015b] that determine the NO<sub>x</sub> emission to fuel consumed ratio and the NO<sub>x</sub> to trace gas emission ratio. Satellite data provide global coverage, which is especially important, as most regions of the world do not have surface-based observational networks.

The Ozone Monitoring Instrument (OMI) on the NASA Aura satellite has provided observations of several key air pollutants since late 2004, a period with significant changes in NO<sub>x</sub> levels for most world regions and cities [e.g., Hilboll et al., 2013; Schneider et al., 2015; Krotkov et al., 2015]. OMI tropospheric column NO<sub>2</sub> data, an effective proxy for the level of surface NO<sub>x</sub> in polluted areas [e.g., Lamsal et al., 2015], show that there were substantial decreases in NO<sub>2</sub> levels over the past decade over large areas of the United States (U.S.), Japan, and many western European countries [e.g., Russell et al., 2012; Castellanos and Boersma, 2012; Duncan et al., 2013; Lamsal et al., 2015; Tong et al., 2015]. During the same period, there were significant changes over

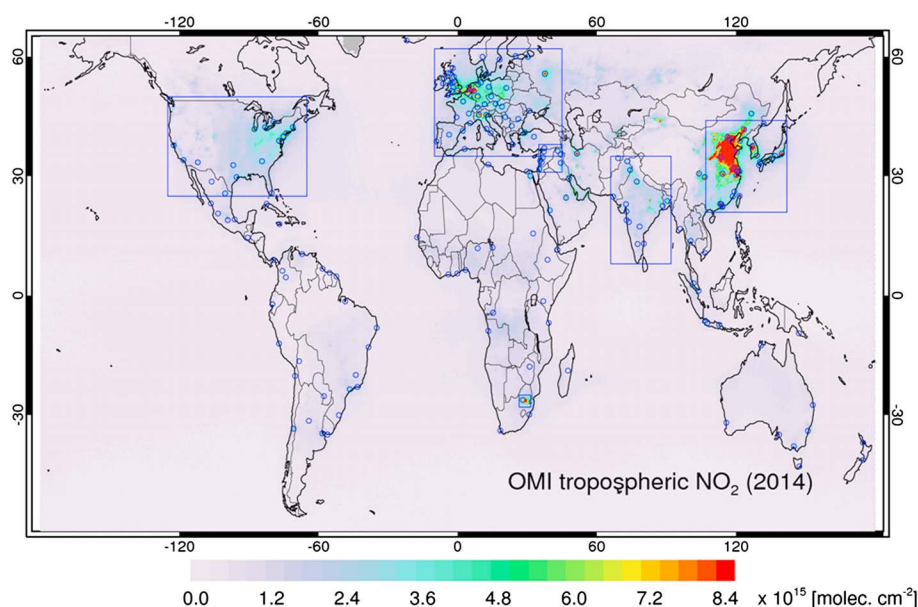


**Figure 1.** OMI NO<sub>2</sub> data ( $\times 10^{15}$  mol/cm<sup>2</sup>; 0.1° latitude  $\times$  0.1° longitude) as an annual average for 2014. The circles represent the cities for which we calculated changes. The boxes indicate specific regions that are presented in section 3.

many regions of the Middle East, India, and China [e.g., Ghude *et al.*, 2011; Lu and Streets, 2012; Wang *et al.*, 2010, 2012; Jin and Holloway, 2015; Lelieveld *et al.*, 2015]. Hilboll *et al.* [2013] combined Global Ozone Monitoring Experiment (GOME) and Scanning Imaging Absorption spectroMeter for Atmospheric CHartographY (SCIAMACHY) data to investigate NO<sub>2</sub> changes for many world regions and 35 cities. While they determined changes using data with a coarser spatial resolution than the OMI data used in the current study, their analysis allowed NO<sub>2</sub> changes to be estimated over a longer period (16 years), pushing the NO<sub>2</sub> data record back to 1996. Schneider *et al.* [2015] used SCIAMACHY data mapped to a 0.25° latitude  $\times$  0.25° longitude grid to estimate changes for 66 world cities from August 2002 to March 2012, ascribing some changes to economic and demographic factors. Typically, however, changes in population are strongly correlated with economic growth, urbanization, energy usage, pollution, and other factors. Lamsal *et al.* [2015] use OMI data mapped to a 0.1° latitude  $\times$  0.1° longitude grid and show that NO<sub>2</sub> exhibits considerable spatial heterogeneity within U.S. cities that is associated with nonuniform changes in emissions from various sources (e.g., industry, power generation, and vehicles).

In this study, we (1) present NO<sub>2</sub> changes from 2005 to 2014 over a larger number of world cities (i.e., 195 cities; Figure 1 and Tables S1–S9 in the supporting information) and with higher spatial resolution (i.e., 0.1° latitude  $\times$  0.1° longitude) data than in previous studies; (2) demonstrate that the OMI data reveal spatial heterogeneity in changes within megacities (i.e., expanding on the work of Lamsal *et al.* [2015]) and often-times allow for the attribution of these changes to large individual sources, such as industrial complexes; and (3) identify a larger number of factors that may cause the observed changes than were considered in previous studies. We find that the changes for the majority of cities appear to be primarily determined by one or more of the following factors: (1) local, regional, and/or country environmental regulations (e.g., the implementation of emission control technology); (2) economic changes and associated changes in energy usage; (3) regional pollution transport; (4) the impact of civil unrest on economic activity and energy usage; and (5) ambitious infrastructure development and mixed efforts to cope with air quality degradation.

Our manuscript is organized as follows. First, we describe the high-resolution OMI data and the analysis method in section 2.1. Using the Seoul megacity (Republic of Korea) as an example, we demonstrate the value of high-resolution satellite data for understanding changes in complex sources regions and attributing those changes to individual sources (section 2.2). We then discuss OMI NO<sub>2</sub> levels and changes by region (Figure 1) in section 3. We present the decreasing changes in Western Europe and the U.S. (section 3.1), which are primarily due to environmental regulation compliance. In section 3.2, we present the increases in South Asia, which are likely associated with intense industrial development and energy production/usage. In

section 3.3, we discuss the complex spatial heterogeneity of changes in China, including decreases in Beijing, Shanghai, Taiwan, and the cities of the Pearl River Delta. In section 3.4, we discuss the possible influence of Chinese  $\text{NO}_x$  emissions on regional  $\text{NO}_2$  levels and changes in Japan and the Korean Peninsula. In section 3.5, we present changes in cities impacted by civil unrest, such as in Libya, Syria, and Iraq. In section 3.6, we summarize our analysis for cities in the tropics and subtropics, which exhibit differences between the wet and dry seasons. In section 3.7, we present changes in the Johannesburg-Pretoria (South Africa) megacity, which is an area with a complex mix of  $\text{NO}_x$  sources and changes.

We use independent information, when available, to provide plausible interpretations of the OMI-observed changes. However, we acknowledge the need for more in depth verification of the causes of the changes as well as the reliability of the independent information, both of which are beyond the scope of this manuscript. Consistency between OMI observations and independent data sources give us some confidence in OMI changes in areas without such independent information. However, the end-user of the data should exercise caution when interpreting changes in areas without independent data as some changes may be due to data artifacts [e.g., *Duncan et al.*, 2014]. The changes for our 195 cities are shown in Tables S1–S9, and the spatial plots and time series are located at <https://airquality.gsfc.nasa.gov/>.

## 2. Description of High-Resolution OMI $\text{NO}_2$ Data and Demonstration of Its Utility

### 2.1. Data Description and Methods

The OMI, a Dutch/Finnish collaboration, collects data approximately once a day at a given location on the Earth's surface between 1300 and 1445 local standard time at a spatial resolution of up to  $13 \text{ km} \times 24 \text{ km}$  with near daily global coverage. The OMI  $\text{NO}_2$  data are tropospheric vertical column densities, the total number of  $\text{NO}_2$  molecules between the tropopause and the Earth's surface per unit area. The data set is generated using spectral variation in backscattered solar radiation in the broad visible spectral window between 405 and 465 nm. The retrieval algorithm used to generate the data includes recent improvements as described in *Bucsela et al.* [2013] and *Lamsal et al.* [2014]. The data are publicly available from the NASA Goddard Earth Sciences Data Active Archive Center (GES DISC; <http://disc.sci.gsfc.nasa.gov>). In this study, we use clear-sky observations (cloud fraction  $< 30\%$ ) and exclude the largest pixels on the swath edges (rows 1–4). We use only rows 5–23, excluding those affected by the row anomaly [*Dobber et al.*, 2008], so as to avoid inconsistent sampling of the data. We map the remaining OMI data pixels onto a  $0.1^\circ$  latitude  $\times$   $0.1^\circ$  longitude grid by calculating an area-weighted average. It is important to note that some variables, such as surface reflectivity and the  $\text{NO}_2$  profile shape, may vary at scales smaller than the OMI pixel size, affecting the retrieved  $\text{NO}_2$  tropospheric vertical column densities [e.g., *Russell et al.*, 2011; *Lamsal et al.*, 2015]. In addition, these variables may change over time. Future retrieval algorithm improvements include the use of observed surface reflectivity from the Moderate Resolution Imaging Spectroradiometer, which should allow for better quantification of the impact of such changes on the changes derived from OMI  $\text{NO}_2$  data.

The multivariate linear regression method that we use for trend estimation is described in *Lamsal et al.* [2015]. It separates the time series of monthly average  $\text{NO}_2$  values into three additive subcomponents: one that is seasonal and time dependent, a linear trend, and a residual. This is particularly useful for estimating changes in regions with significant changes in  $\text{NO}_2$  levels as the time-dependent seasonal subcomponent can be non-trivial and influence a linear trend if not accounted for properly [*Lamsal et al.*, 2015]. All changes reported in this manuscript are the linear trend subcomponents in the units of percent/decade, which reflect the percent changes over our study period, 2005 to 2014. For most cities, the residual subcomponent is small ( $< 10\%$ ), explaining little of the total variance. When the residual subcomponent is larger and varies over the study period, we explicitly discuss these short-term, notable variations and attempt to attribute them to, for instance, meteorology, civil unrest, and economic growth or contraction. Not all variations in the residual term can be explained. For some cities, the residual subcomponent may include contributions from the seasonal subcomponent if the seasonal cycle is not represented well by the intraannual sine and cosine harmonic series [*Randel and Cobb*, 1994] used in our regression method. Therefore, time series of the residual terms could still contain seasonality. This does not affect the estimated trend, but large variations could increase the uncertainty in the estimated trend.

We selected 5 regions and 195 cities based on population, location within regions with interesting spatial heterogeneity in changes, and location so as to achieve spatial coverage of the globe. A change for each world

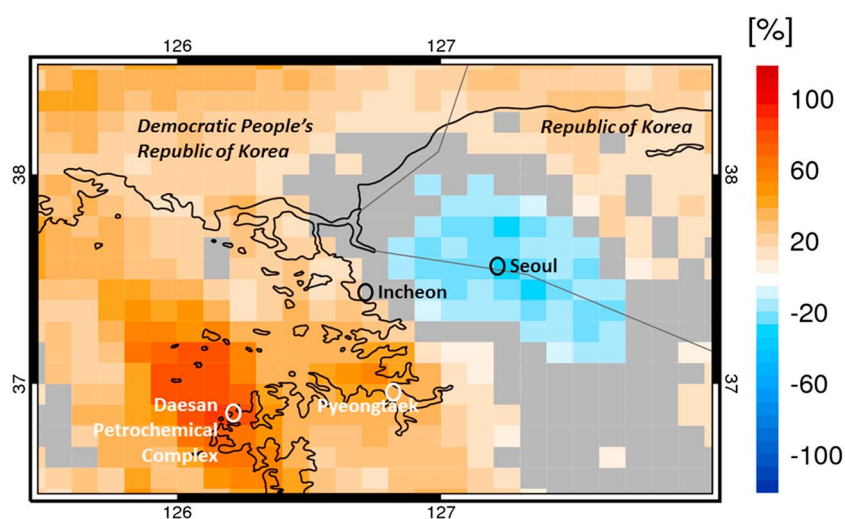


**Figure 2.** The change (%) in OMI NO<sub>2</sub> data (0.1° latitude × 0.1° longitude) between 2005 and 2014 for the Seoul metropolitan area. Gray areas represent where there are no statistically significant changes. The light gray lines represent rivers. Latitudes and longitudes are given on the axes.

city is reported as the average of OMI NO<sub>2</sub> data within a 0.3° latitude × 0.3° longitude box centered over the city. However, in all spatial illustrations in this manuscript, changes are shown for 0.1° latitude × 0.1° longitude boxes. Changes for all cities are shown by region in Tables S1–S9.

Our strategy for identifying the potential cause(s) of OMI NO<sub>2</sub> changes over individual cities is as follows. First, we researched the literature for attribution studies to identify one potential cause of the change for each of the 195 cities. For instance, NO<sub>2</sub> decreases in many western countries are attributed to environmental regulations on NO<sub>x</sub> emissions. We sorted all cities into five categories: (1) environmental regulations; (2) economic changes; (3) regional pollution transport; (4) civil unrest; and (5) infrastructure development. In the absence of a previous study, we used our judgment to identify the potential cause. For some smaller cities, we simply assigned them to the category of economic changes, which may include population changes. Second, we searched for independent data to support/refute the potential cause. Such data do not exist (or are not readily available) for some smaller cities, particularly in the tropics and subtropics. Based on our analysis of the independent data, we moved several cities between the five categories. Third, we investigated the possibility that multiple factors influenced the change for a given city and, again, searched for independent data to support/refute these other potential causes. We used the following independent data sources: (1) international databases, such as for economic indicators and energy usage, (2) national reports on environmental regulations, energy usage, infrastructure development, etc., (3) papers in the scientific literature, (4) satellite data of land use, including high-resolution data to identify point sources and the timing of infrastructure development, (5) news reports, and (6) business reports from private companies.

## 2.2. Spatial Heterogeneity and Value of High Resolution NO<sub>2</sub> Data

With a case study of the Seoul megacity (Republic of Korea), we explicitly demonstrate the value of a high-resolution observing strategy for differentiating changes among individual NO<sub>x</sub> sources in complex source regions, a task that is not possible with coarse-resolution data. There is a complex spatial distribution of changes for the Seoul metropolitan area (Figure 2). The largest decreases on the Korean Peninsula occur in Seoul (−15.0 ± 12.5%) and are likely associated with Korea's NO<sub>x</sub> emission control efforts [e.g., Wang *et al.*, 2014]. Surface air quality monitors in Seoul show an average NO<sub>2</sub> decrease of 11% from 2004 to 2013 [Min. Environ, 2015]. The largest increases occur southwest of Seoul, which includes (1) the ports of Pyeongtaek, Daesan, and Incheon, (2) the Incheon Free Economic Zone, on which infrastructure development began in 2003 and continues today [Free Economic Zone (FEZ), 2003, 2015], (3) the Incheon International Airport, one of the world's busiest airports and main airport for Seoul, that has rapidly been expanding capacity over the last decade [Jin, 2013; Airport Technology, 2015], and (4) the Daesan Petrochemical Complex, which has been rapidly expanding operations since 2005 [Total, 2015]. The largest change that occurs over open



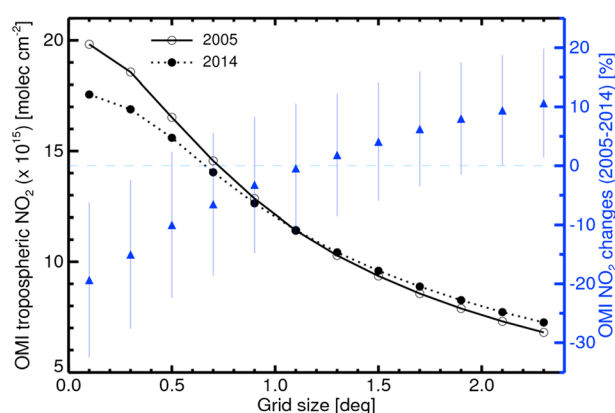


**Figure 3.** OMI  $\text{NO}_2$  levels ( $\times 10^{15}$  mol/ $\text{cm}^2$ ) for the Seoul metropolitan area in 2005 (solid black line) and 2014 (dotted black line) as functions of spatial resolution (degrees) centered over central Seoul. The blue triangles show changes (%) in  $\text{NO}_2$  levels as a function of spatial resolution between 2005 and 2014; vertical bars represent the 95% confidence interval.

are negative (at the 95% confidence level) for spatial resolutions  $< 0.3^\circ$  latitude  $\times$   $0.3^\circ$  longitude, insignificant for resolutions between  $0.5^\circ \times 0.5^\circ$  and  $2.1^\circ \times 2.1^\circ$ , and positive (at the 95% confidence level) for resolutions  $> 2.2^\circ \times 2.2^\circ$ . This example demonstrates that useful information on changes in various emission sources and energy consumption patterns within the Seoul metropolitan area is lost at coarse spatial resolutions.

waters near Daesan may be associated with increased shipping servicing the petrochemical complex. Though the changes over Daesan and surrounding waters are largest, the emission control efforts in Seoul likely offset, to some degree, the probable rising emissions from the growing Incheon Free Economic Zone and Incheon International Airport. Surface air quality monitors in Incheon show no  $\text{NO}_2$  change on average from 2004 to 2013 [Min. Environ, 2015].

Figure 3 demonstrates how the city's change is highly dependent on spatial resolution. The changes are calculated with grid boxes of various sizes centered on central Seoul. The changes

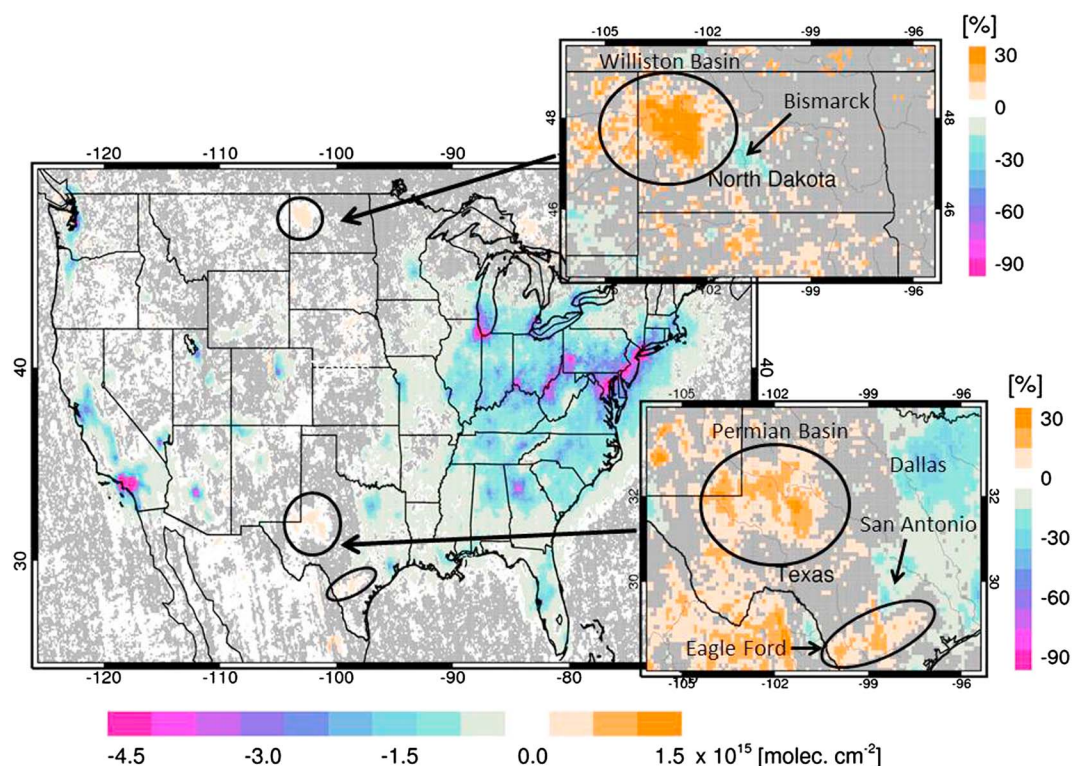


**Figure 4.** (left center) OMI  $\text{NO}_2$  absolute changes ( $\times 10^{15}$  mol/ $\text{cm}^2$ ;  $0.1^\circ$  latitude  $\times$   $0.1^\circ$  longitude) from 2005 to 2014 over the U.S. (inset top right) Change (%) over North Dakota. (inset bottom right) Change (%) over Texas. The areas of large percent increases over northern Mexico, which has a relatively low population density, low  $\text{NO}_x$  emissions, and sparse oil and natural gas extraction activities, are very small absolute changes as shown in the figure (left center). Gray areas represent where there are no statistically significant changes.

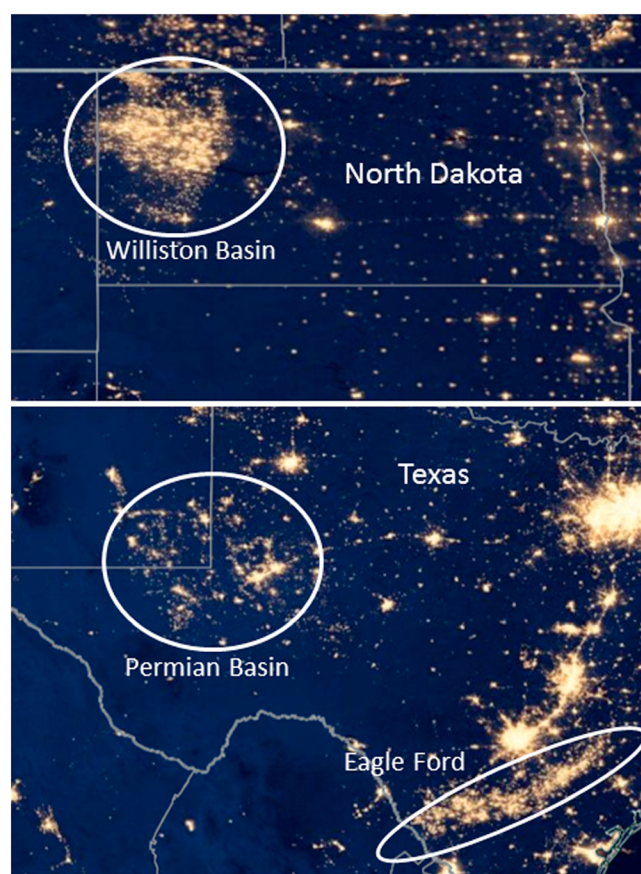


**Figure 5.** Lights at night data from Suomi NPP VIIRS for (top) North Dakota and (bottom) western Texas.

### 3. Changes in NO<sub>2</sub> Levels Around the Globe

In the subsections that follow, we present changes for cities and regions in the U.S. and Europe, South Asia, China, Japan, and the Republic of Korea, Middle East, tropics and subtropics, and South Africa.

#### 3.1. Implementation of Emission Control Technology: Europe and United States

Prior studies using satellite data indicate that NO<sub>2</sub> levels decreased sharply over the last decade in many countries, such as the U.S., Japan, Australia, New Zealand, and those in Western Europe. This decrease resulted from a combination of the implementation of emission control devices on thermal power plants, the shuttering of inefficient plants, and stricter vehicle emission standards [Kim *et al.*, 2006; McFarlane, 2009; Castellanos and Boersma, 2012; Russell *et al.*, 2012; Schneider and van der A, 2012; Zhou *et al.*, 2012; Duncan *et al.*, 2013; Lamsal *et al.*, 2015; Tong *et al.*, 2015].

OMI NO<sub>2</sub> levels are generally decreasing over the continental U.S. ( $\sim 25\text{--}55\%$ ; Table S1), as discussed in detail in Lamsal *et al.* [2015], but three areas of the central U.S. show significant absolute increases ( $>0.5 \times 10^{15} \text{ mol/cm}^2$ ; Figure 4). These increases (10–30%) may be associated with the rapid expansion of oil and natural gas extraction activities over the Williston Basin of western North Dakota and the Permian Basin and Eagle Ford shale play areas of western Texas [U.S. Energy Information Administration (USEIA), 2013, 2015a]. The growth in NO<sub>x</sub> emissions is associated with the (1) consumption of fossil fuels by the heavy machinery and vehicles used to extract and transport the oil and natural gas and (2) other processes, such as flaring. Lights associated with these activities are observable from space, such as the Visible Infrared Imaging Radiometer Suite (VIIRS) on the Suomi National Polar-orbiting Partnership (NPP) satellite [Hillger *et al.*, 2013]. There is a general match of shape of the area of NO<sub>2</sub> increases with the distribution of lights in all three regions (Figure 5), which suggests that the increases are associated with increased NO<sub>x</sub> emissions from the oil and natural gas extraction activities. Increases in NO<sub>2</sub> levels in other major oil and natural gas production regions, such as the Marcellus in Pennsylvania, New York, and West Virginia, are not clear and may be masked by the large decreases that occurred because of colocated NO<sub>x</sub> emission reductions from cars and power plants.

There are also large decreases in OMI NO<sub>2</sub> levels from 2005 to 2014 over most European cities (Table S2), which are likely due to tightening vehicle emission standards by level and date [Euro, 2007]. The largest decreases ( $\sim 45\text{--}55\%$ ) occur over the major cities of the Iberian Peninsula (Madrid and Barcelona (Spain) and Lisbon (Portugal)) and Athens (Greece). Large absolute decreases occur over other major cities, such as Paris (France), London (United Kingdom), Moscow (Russia), and those in the Netherlands, Belgium, and the industrialized Po River Valley (Italy) and Ruhr region (Germany). In fact, there are no large absolute increases over European cities though there are modest ones over areas of Eastern Europe (e.g., in Poland and Ukraine) and a small area near Bremen (Germany; Figure 6); Bremen itself has no significant change. The cause of the increase ( $>30\%$ ) over IJsselmeer and Wattenmeer in the Netherlands is likely a retrieval artifact [Boersma *et al.*, 2011].



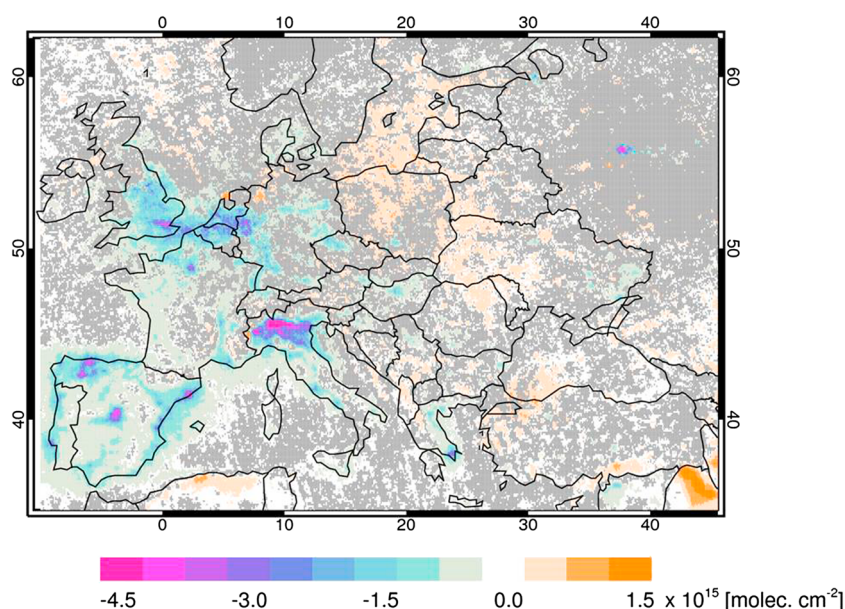


**Figure 6.** OMI NO<sub>2</sub> absolute change ( $\times 10^{15}$  mol/cm<sup>2</sup>; 0.1° latitude  $\times$  0.1° longitude) from 2005 to 2014 over Europe. Gray areas represent where there are no statistically significant changes.

In contrast to several earlier studies [Russell *et al.*, 2012; Castellanos and Boersma, 2012], we find no clear evidence of the impact of the 2008–2009 recession [e.g., United States Bureau of Labor Statistics (USBLS), 2012] for U.S. or European cities in our OMI NO<sub>2</sub> data. However, slow economic recovery in some countries, such as Spain and Greece, likely contributed to the overall NO<sub>2</sub> decrease. The time series in OMI data for most U.S. cities show a sharp decrease in NO<sub>2</sub> levels from 2005 to 2008, followed by a smaller or no decrease after 2009, as reported by Lamsal *et al.* [2015]. Russell *et al.* [2012], Lamsal *et al.* [2015], and Tong *et al.* [2015] discuss that the signal of the recession in the U.S. is convolved with emission controls occurring at the same time. For instance, Duncan *et al.* [2013] present OMI NO<sub>2</sub> changes over U.S. thermal power plants, which were implementing emission control devices around the time of the recession to comply with the Clean Air Interstate Rule issued by the U.S. Environmental Protection Agency. In Europe, Castellanos and Boersma [2012] discuss the impact of the economic recession, but they included data only through 2011. We find that the times series of OMI NO<sub>2</sub> data show fairly consistent downward changes in European cities, such as London, Rome, Madrid, and Paris, with little or no differentiation among the changes before and after the recession as in the U.S.

### 3.2. Economic Growth: South Asian Cities and Emission Hot Spots

South Asian economies have been strong for the last decade with generally large growth in energy consumption, which may explain the observed increases of NO<sub>2</sub> levels (Figure 7). The Gross Domestic Products (GDP; constant 2005 U.S. dollar) of Pakistan, India, and Bangladesh increased by 38%, 92%, and 71%, respectively, from 2005 to 2014 [World Bank, 2015]. According to the World Health Organization's (WHO) database [WHO, 2014], a number of cities in South Asia have the poorest air quality in the world [Lu *et al.*, 2011; Lu and Streets, 2012]. While there are numerous pollution sources, vehicle traffic has been previously noted as a major contributor to pollution in most cities in India [e.g., Guttikunda *et al.*, 2014]. The Society of Indian Automobile Manufacturers (<http://www.siamindia.com>) reports a 61% increase in domestic autosales from 2009 to 2015. Regardless of emission technology, ubiquitous traffic congestion in many of the world's cities results in idling vehicles and concomitant high NO<sub>x</sub> emissions. Nevertheless, OMI data show that NO<sub>2</sub> levels in South Asia, as well as other tropical and subtropical countries (section 3.6), are lower than levels in industrialized countries (section 3.1 and Figure 1). This may reflect differences in (1) NO<sub>x</sub> lifetime (i.e., longer in winter at higher latitudes than lower latitudes), (2) energy sources (e.g., biomass versus fossil fuel) and combustion temperature, (3) vehicle type and efficiency, and (4) per capita energy consumption between emerging and industrialized economies [e.g., Lamsal *et al.*, 2013; Dickerson *et al.*, 2002, and references therein; World Dev. Ind, 2015].



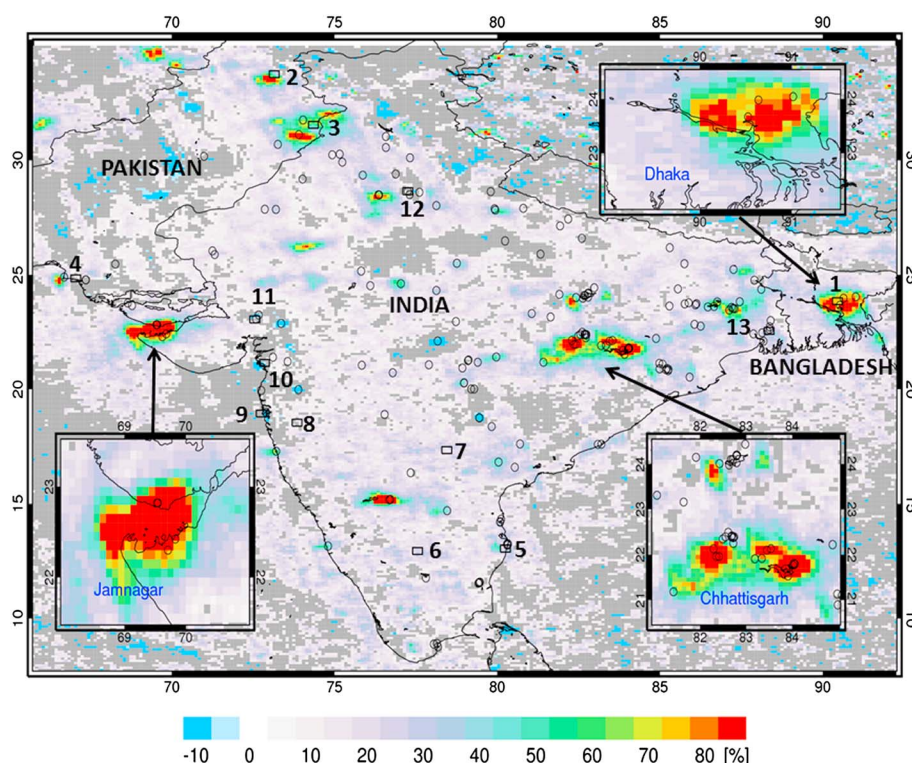


**Figure 7.** Changes (%) of OMI NO<sub>2</sub> data (0.1° latitude × 0.1° longitude) between 2005 and 2014. Gray areas represent where there are no statistically significant changes. The insets are of the Jamnagar Refining and Petrochemical Complex in western India, Dhaka (Bangladesh) and surrounding area, and Chhattisgarh, an area rich in coal and with numerous thermal power plants (circles). The numbers next to boxes correspond to cities given in Table 1.

There is a mix of changes in OMI NO<sub>2</sub> levels over South Asian cities (Figure 7 and Tables 1 S3), though many are large increases, likely reflecting the strong economic growth and increased energy usage of this region. The capitals of Pakistan, India, and Bangladesh are located on the fertile, densely populated Indo-Gangetic Plain, the most heavily polluted region of South Asia, extending from northeastern Pakistan, across most of northern India, and into Bangladesh. The largest change in OMI NO<sub>2</sub> levels of any major world city in

our study (Tables S1–S9) occurs over Dhaka (Bangladesh;  $79.3 \pm 13.9\%$ ), which was also reported in previous studies [Schneider and van der A, 2012; Hilboll et al., 2013]. Other notable increases (Table 1 and Figure 8) occur in Islamabad (Pakistan;  $46.7 \pm 11.7\%$ ), Kolkata in eastern India ( $26.6 \pm 10.4\%$ ), and southern India, including the cities of Chennai, Bengalura, and Hyderabad (17–27%). In contrast, Karachi (Pakistan), New Delhi (India), and cities in the Mumbai-Gujarat industrial corridor on the west coast of India, including Pune, Mumbai, Surat, and Ahmedabad, have insignificant changes (Figure 7 and Table 1).

Despite intensive economic growth of the last decade, we observe

**Table 1.** OMI NO<sub>2</sub> Changes (%; 2005–2014) for South Asian Cities

City <sup>a</sup>	Change (%)
<i>Bangladesh</i>	
1. Dhaka	$79.3 \pm 13.9$
<i>Pakistan</i>	
2. Islamabad	$46.7 \pm 11.7$
3. Lahore	$52.7 \pm 15.4$
4. Karachi	$4.81 \pm 10.4$
<i>India</i>	
5. Chennai	$24.9 \pm 11.5$
6. Bengalura	$23.3 \pm 8.5$
7. Hyderabad	$16.8 \pm 10.8$
8. Pune	$11.1 \pm 11.5$
9. Mumbai	$-6.83 \pm 10.1$
10. Surat	$-4.57 \pm 7.5$
11. Ahmedabad	$-2.39 \pm 7.5$
12. New Delhi	$6.13 \pm 13.7$
13. Kolkata	$26.6 \pm 10.4$

<sup>a</sup>City locations are shown in Figure 7.

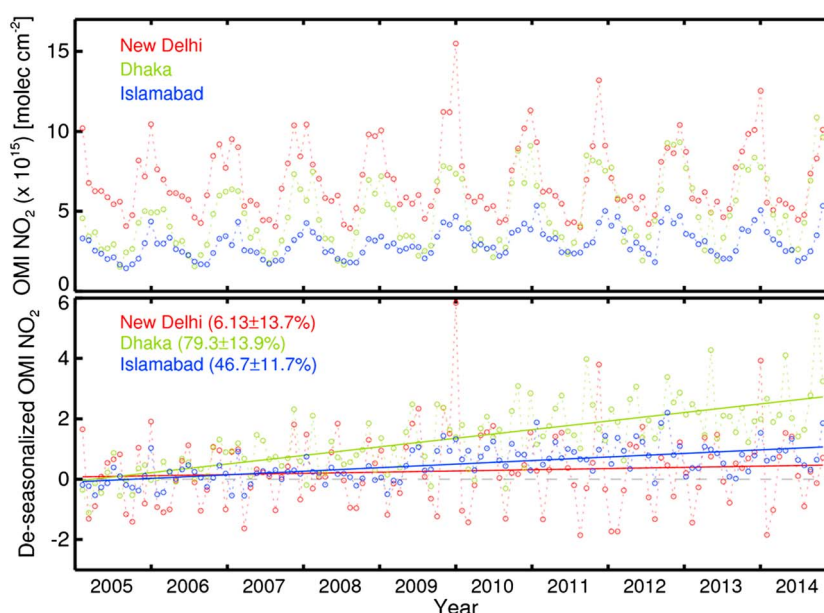


**Figure 8.** (top) Monthly OMI NO<sub>2</sub> data ( $\times 10^{15}$  mol/cm<sup>2</sup>) over New Delhi (India), Dhaka (Bangladesh), and Islamabad (Pakistan). (bottom) Deseasonalized (i.e., linear + residual terms), monthly OMI NO<sub>2</sub> data ( $\times 10^{15}$  mol/cm<sup>2</sup>) with relative trends.

smaller NO<sub>2</sub> changes from 2005 to 2014 than those of *Ghude et al.* [2008, 2011] and *Ramachandran et al.* [2013], which we attribute to referencing different base years and using finer resolution data in our analysis. We find spatial heterogeneity in the changes in the cities of New Delhi and the Mumbai-Gujarat industrial corridor with decreases or insignificant changes in the city centers and increases outside of the city centers. This spatial pattern may occur for a variety of reasons, including limited growth due to physical space constraints within city centers, efforts to reduce emissions in city centers (e.g., commuter rail development in Mumbai, Surat.) [*Min. Urb. Develop.*, 2015] and/or the growth or relocation of industry and power generation facilities (e.g., for cheaper operating costs) away from the city centers. We find a similar spatial pattern (i.e., decrease within the city center and increases surrounding the city center) outside of South Asia, such as in Cairo (Egypt) and Riyadh (Saudi Arabia).

Several researchers have previously reported South Asian emission hot spots (i.e., urban and industrial areas and thermal power plants) and increasing NO<sub>2</sub> changes, using data with relatively coarse spatial resolutions from a number of satellite sensors [*Ghude et al.*, 2008; *Lu and Streets*, 2012; *Ramachandran et al.*, 2013; *ul-Haq et al.*, 2014]. The largest hot spots are found over thermal power plants [*Lu and Streets*, 2012; *Prasad et al.*, 2012], such as the Chhattisgarh region (Figure 7) because coal is fueling India's economic boom [e.g., *Guttikunda and Jawahar*, 2014; *USEIA*, 2015b]. *Lu and Streets* [2012] used NO<sub>2</sub> data from the GOME, SCIAMACHY, OMI, and GOME-2 instruments to estimate that NO<sub>x</sub> emissions from Indian power plants increased by at least 70% from 1996 to 2010. Coal production and consumption in India increased by ~50% over our study period [*Min. Coal*, 2014], which is consistent with changes in Chhattisgarh, an area rich in coal and with numerous thermal power plants.

We find the largest change ( $> +100\%$ ) in OMI NO<sub>2</sub> levels in India over the Jamnagar Refining and Petrochemical Complex in western India (Figure 7). This complex is the world's largest oil refining complex that has undergone major expansion in the last decade [*Min. Petrol. and Natural Gas*, 2015]. The large area of increase extends across the Bay of Kutch, which may result from increased shipping activities associated with the complex and into the Mundra Port area, which includes the new Mundra Ultra Mega Power Plant (4000 MW capacity) that came online in 2012–2013 [*Min. Power*, 2015].

### 3.3. Economic Growth in China and Uneven Emission Control Efforts

China's economy has substantially increased over the last few decades [e.g., *Lee and Hong*, 2012] with the country's GDP (constant 2005 U.S. dollar) increasing by 132% from 2005 to 2014 and annual growth rates

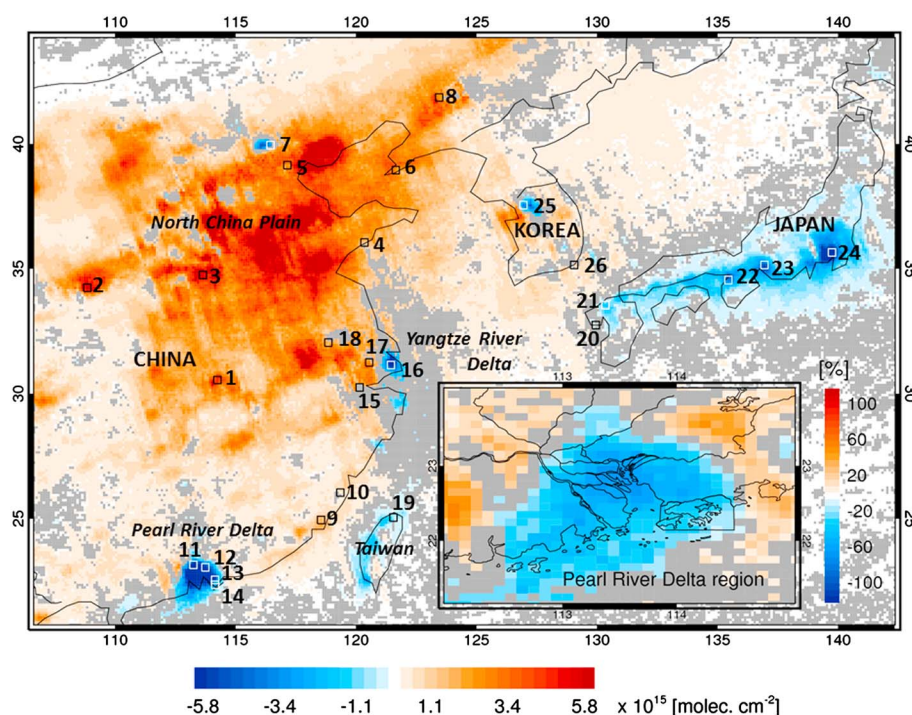


**Figure 9.** The change ( $\times 10^{15}$  mol/cm<sup>2</sup>;  $0.1^\circ$  latitude  $\times 0.1^\circ$  longitude) in OMI NO<sub>2</sub> levels from 2005 to 2014. Gray areas represent where there are no statistically significant changes. The numbers correspond to cities given in Table 2. (inset) The linear change (%) in OMI NO<sub>2</sub> data from 2005 to 2014 for the PRD.

**Table 2.** OMI NO<sub>2</sub> Changes (%; 2005–2014) for Chinese Cities

City <sup>a</sup>	Change (%)
<i>North China Plain</i>	
1. Wuhan	42.3 $\pm$ 20.1
2. Xi'an	39.3 $\pm$ 16.5
3. Zhengzhou	35.3 $\pm$ 16.9
4. Qingdao	18.6 $\pm$ 21.3
5. Tianjin	21.0 $\pm$ 15.4
6. Dalian	39.6 $\pm$ 15.9
7. Beijing	−10.3 $\pm$ 13.1
8. Shenyang	27.9 $\pm$ 19.7
<i>SE China Coast</i>	
9. Quanzhou	49.6 $\pm$ 14.4
10. Fuzhou	12.2 $\pm$ 11.1
<i>Pearl River Delta</i>	
11. Guangzhou	−43.5 $\pm$ 14.7
12. Dongguan	−46.0 $\pm$ 10.9
13. Shenzhen	−41.8 $\pm$ 9.9
14. Hong Kong	−28.4 $\pm$ 10.7
<i>Yangtze River Delta</i>	
15. Hangzhou	−0.91 $\pm$ 19.9
16. Shanghai	−30.0 $\pm$ 13.9
17. Suzhou	11.2 $\pm$ 15.0
18. Nanjing	14.5 $\pm$ 15.2
<i>Taiwan</i>	
19. Taipei	−29.2 $\pm$ 12.0

<sup>a</sup>City locations are shown in Figure 9.

of 7–14% [World Bank, 2015]. This growth is fueled by the country's cheap and abundant coal [e.g., Li and Leung, 2012; Liu et al., 2015a, 2015b; USEIA, 2015c]. Vehicle sales surged in the last decade, surpassing 20 million units sold in 2013 [Chinese Assoc. of Auto. Manuf., 2014]. China's economy grew at the expense of its air quality [e.g., Richter et al., 2005; Chan and Yao, 2008; Fang et al., 2009; Wang et al., 2010; Lei et al., 2011; Wang et al., 2012; Lin et al., 2013], including NO<sub>x</sub> pollution [e.g., Zhang et al., 2007; Zhang et al., 2009; Liu et al., 2015a, 2015b]. There are large increases in OMI NO<sub>2</sub> levels over China, particularly the North China Plain (Figure 9 and Tables 2 and S4).

Despite China's strong economic growth, we find large decreases in OMI NO<sub>2</sub> levels over Beijing, Shanghai, Taiwan, and the Pearl River Delta (PRD), which includes the cities of Hong Kong, Shenzhen,



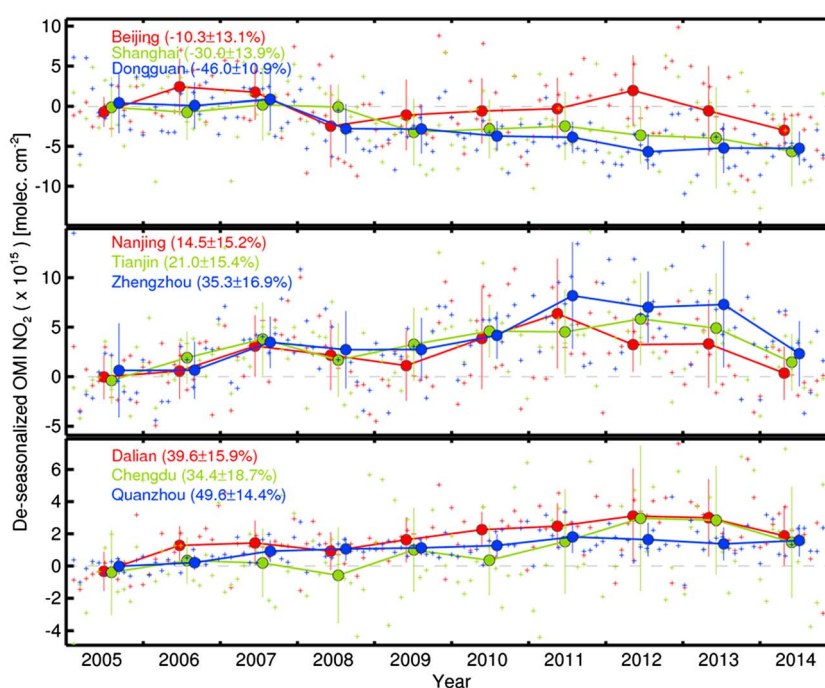


**Figure 10.** Deseasonalized (i.e., linear + residual terms) OMI  $\text{NO}_2$  data ( $\times 10^{15}$  mol/cm<sup>2</sup>) for nine Chinese cities. Monthly and annual average values are shown as pluses (+) and circles, respectively. The vertical bars on the annual average values represent the standard deviation for a given year.

Dongguan, and Guangzhou (Figure 9 and Table 2). This finding is consistent with *Jin and Holloway* [2015], who report insignificant or decreasing changes using a different version of OMI  $\text{NO}_2$  data. These decreases are likely the result of efforts within some cities and regions of China to reduce pollutant emissions, which have resulted in decreases in surface  $\text{NO}_x$  levels [e.g., *Lu et al.*, 2010, 2011; *Li et al.*, 2010; *Gu et al.*, 2013]. For instance, the Shanghai Environmental Protection Bureau has aggressively worked with local industry and thermal power facilities and eliminated highly polluting vehicles so that surface  $\text{NO}_x$  levels decreased by  $\sim 17\%$  from 2008 to 2011 [*Shanghai Environmental Bulletin (SEB)*, 2012]. The neighboring cities (Nanjing, Suzhou, and Hangzhou) all have insignificant changes (Table 2) possibly because of their own local emission control efforts or their own increases in  $\text{NO}_x$  emissions were offset by the decreases in Shanghai. Recently, Shanghai and three neighboring provinces in the Yangtze River Delta agreed to coordinate their efforts to curb pollution [*Yue*, 2014]. As another example, the Guangdong-Hong Kong-Macao PRD Regional Air Quality Monitoring Network came online in 2005; surface  $\text{NO}_x$  levels decreased by 20% from 2006 to 2014 through cooperation across the PRD to control  $\text{NO}_x$  emissions (e.g., thermal power plants, and vehicles), phase out old industry, etc. [*Zhong et al.*, 2013; *PRDAIR*, 2014].

The emissions reductions in Beijing and Shanghai may have been more substantial than their OMI changes indicate since the lifetime is long enough for  $\text{NO}_2$  to be transported from neighboring regions where increases in  $\text{NO}_2$  levels were observed (Figure 9 and Table 2). For Beijing, the decrease in  $\text{NO}_2$  levels is phenomenal given that the metropolitan area quadrupled in area in the last decade [*Jacobson et al.*, 2015]. Given the increases over the marine area between the mainland and Taiwan, it is possible that changes in  $\text{NO}_2$  levels over the west coast of Taiwan were influenced by the import of mainland  $\text{NO}_2$ . Mainland coastal cities near Taiwan have large increases in  $\text{NO}_2$  levels (e.g., Quanzhou and Fuzhou (Table 2)).

We find variability in the evolution of  $\text{NO}_2$  levels in China's cities (Figure 10). Beijing shows lower  $\text{NO}_2$  levels in 2008, which may reflect the substantial emission controls that were put in place for the 2008 Olympic Games [e.g., *Witte et al.*, 2011]. In contrast, both Shanghai and Dongguan in the PRD show steady declines after 2007. For cities with increases, most show either steady growth in  $\text{NO}_2$  levels over time (e.g., Dalian, Chengdu, and Quanzhou) or plateau around 2011 (e.g., Zhengzhou, Tianjin, and Nanjing). Almost all cities show a decrease in  $\text{NO}_2$  levels in 2014. *Krotkov et al.* [2015] report that the OMI  $\text{NO}_2$  level (taken as a regional average over China)



**Table 3.** OMI NO<sub>2</sub> Change (%) 2005–2014 for Japan and the Republic of Korea

City <sup>a</sup>	Change (%)
<i>Japan</i>	
20. Nagasaki	−1.28 ± 12.2
21. Fukuoka	−25.8 ± 9.3
22. Osaka	−39.0 ± 9.0
23. Nagoya	−43.0 ± 8.8
24. Tokyo	−38.2 ± 8.2
<i>Korea</i>	
25. Seoul	−15.0 ± 12.5
26. Busan	3.30 ± 9.9

<sup>a</sup>City locations are shown in Figure 9.

leveled off in 2012–2013 and decreased in 2014. The cause of this plateau may be associated with emission control efforts and/or the enforcement of existing environmental regulations [e.g., Blanchard and Stanway, 2015].

### 3.4. Japan and Republic of Korea: Possible Reduced Effectiveness of Local NO<sub>x</sub> Emission Controls by Rising Regional Pollution

There are large decreases in OMI NO<sub>2</sub> levels over Japan and the Republic of

Korea (Figure 9 and Tables 3 and S5), consistent with national environmental regulations [Kurokawa *et al.*, 2013]. However, the OMI data suggest that the effectiveness of their local NO<sub>x</sub> emission control strategies may have been diminished by increasing transboundary transport of NO<sub>x</sub> pollution from China. China's pollution is known to negatively impact air quality in countries downwind [e.g., Takashima *et al.*, 2011; Shin *et al.*, 2012; Akimoto *et al.*, 2015]. Lee *et al.* [2014] used a combination of satellite NO<sub>2</sub> data, including from OMI, and a model to demonstrate the influence of Chinese NO<sub>x</sub> emissions on NO<sub>2</sub> levels in adjacent marine areas, Japan, and the Korean Peninsula. They find that the greatest influence occurs in spring when frequent, fast moving synoptic disturbances quickly transport large amounts of NO<sub>x</sub>. However, they report that the seasonal average contribution of Chinese NO<sub>x</sub> emissions to NO<sub>2</sub> levels are at a maximum in winter and a minimum in summer over the Republic of Korea (67% in winter and 30% in summer) and Japan (35% in winter and 2% in summer) because of seasonal variations in the NO<sub>x</sub> lifetime. The findings of Lee *et al.* [2014] are consistent with the increases in OMI NO<sub>2</sub> levels over open waters (i.e., Yellow Sea and East China Sea) between China and the downwind countries (Figure 9) and the large increase over the Democratic People's Republic of Korea, a country with relatively low NO<sub>x</sub> emissions.

The decreases are large for many Japanese cities, including Tokyo, Nagoya, and Osaka (Table 3). This is consistent with surface NO<sub>x</sub> observations that show a large decline after 2006 [Wakamatsu *et al.*, 2013]. However, the changes are weaker in western Japan, including the cities of Fukuoka and Nagasaki, possibly because of disproportionately greater influence of Chinese NO<sub>x</sub> emissions. This inference is consistent with population data, which is typically correlated with NO<sub>x</sub> emissions. Fukuoka's change is more negative than Nagasaki's. Fukuoka is Japan's fourth largest city with a population of 5.6 million in the metropolitan area, while Nagasaki's population is less than half a million. That is, Chinese NO<sub>x</sub> possibly contributes substantially more to total NO<sub>2</sub> levels over Nagasaki than Fukuoka, and thus could have more effectively undermined local control efforts in Nagasaki. However, this hypothesis would need to be confirmed by a study using a model of chemistry and transport.

Despite environmental regulations on local NO<sub>x</sub> emissions, the only large areas of decreases over the Korean Peninsula are in the heavily populated (~26 million) Seoul megacity (Figure 2) and Daegu (2.5 million) in the southern portion of the country (Figure 9). The changes over Busan are insignificant, though surface air quality monitors in both Busan and Daegu report NO<sub>2</sub> decreases of 13% and 12%, respectively, from 2004 to 2013 [Min. Environ, 2015]. The changes over the rest of the Korean Peninsula, including the Democratic People's Republic of Korea, are insignificant or positive, possibly indicating the influence of Chinese NO<sub>x</sub> emissions [Lee *et al.*, 2014]. Chinese coastal cities nearest Korea have large increases (e.g., Qingdao and Tianjin (Table 2)). The highest increases on the Korean Peninsula occur southwest of Seoul and are most likely associated with growth in local industrial activity (section 2.2).

### 3.5. Middle East and Civil Unrest

There is considerable spatial heterogeneity in OMI NO<sub>2</sub> levels and changes over the Middle East (Figure 11 and Table S6) which may be associated with the competing influences of economic growth, emission regulations, and the damaging impact of civil unrest (i.e., a reduction in NO<sub>x</sub> emissions) [Lelieveld *et al.*, 2015]. The large increases in OMI NO<sub>2</sub> levels over Baghdad (Iraq; 67.7 ± 10.9%) and Tehran (Iran; 25.7 ± 20.6%) are

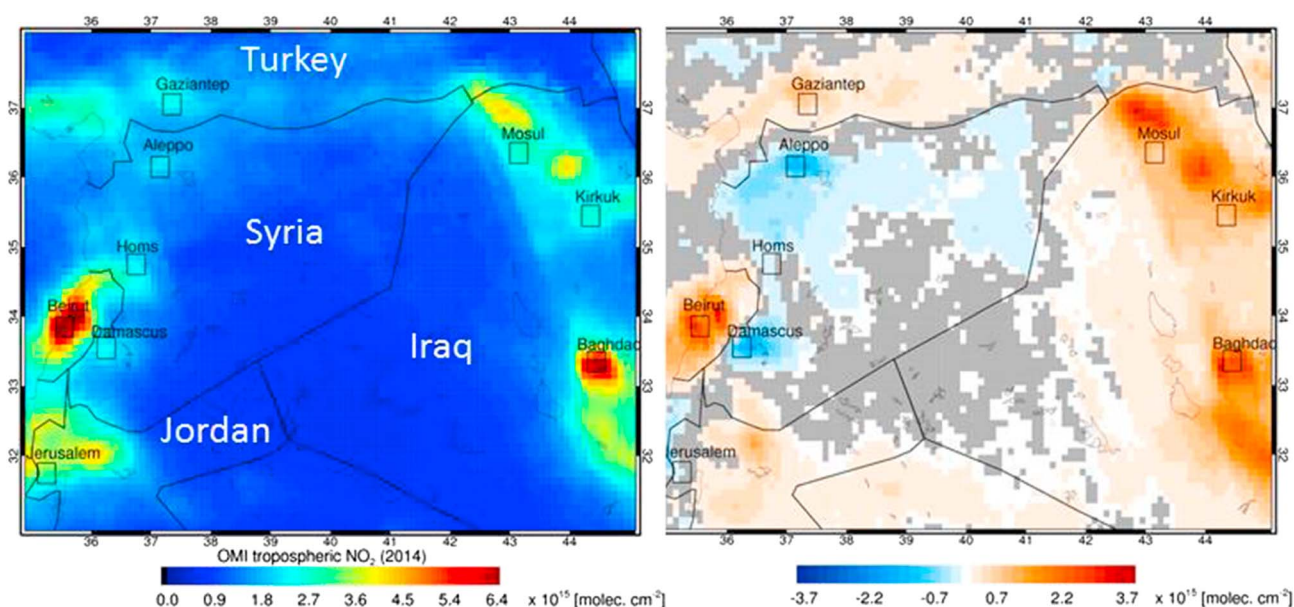


**Figure 11.** (left) OMI  $\text{NO}_2$  data ( $\times 10^{15}$  mol/ $\text{cm}^2$ ;  $0.1^\circ$  latitude  $\times 0.1^\circ$  longitude) as an annual average for 2014 over the Near East. (right) The absolute difference of annual average OMI  $\text{NO}_2$  data ( $\times 10^{15}$  mol/ $\text{cm}^2$ ) between 2005 and 2014. Gray areas represent where there are no statistically significant changes.

consistent with GDP growth (i.e., 67% and 21%, respectively; constant 2005 U.S. dollar) from 2005 to 2014 [World Bank, 2015]. Other large increases ( $>15\%$ ) occur over Kabul (Afghanistan;  $58.6 \pm 13.4\%$ ), Kuwait City (Kuwait;  $17.6 \pm 8.1\%$ ), Mecca (Saudi Arabia;  $23.4 \pm 11.4\%$ ), Mosul (Iraq;  $44.3 \pm 11.8\%$ ), and Kirkuk (Iraq;  $59.6 \pm 12.3\%$ ). There are also increases over parts of the Persian Gulf (Figure S3), which is consistent with Krotkov *et al.* [2015], who note a 20% increase in OMI  $\text{NO}_2$  levels over the last decade. As an aside, the  $\text{NO}_2$  levels in Tehran (metropolitan area population of  $\sim 14$  million) are notable in that they are regularly very high in winter ( $> 30 \times 10^{15}$  mol/ $\text{cm}^2$ ), higher than any other city in this study. The high  $\text{NO}_2$  levels may result from high  $\text{NO}_x$  emissions and wintertime inversions that are exacerbated by topography—mountains surround approximately three quarters of the city [Mohammadi *et al.*, 2012].

**Libya (unrest in 2011).** Civil war began in early 2011 and continued through October. Libya's GDP decreased by 60% (constant 2005 U.S. dollar) from 2010 to 2011 and did not recover completely to prewar levels [World Bank, 2015]. The OMI data show a clear depression in  $\text{NO}_2$  levels in 2011 (Figure 12), which may be related to the unrest. The change (2005–2014) in Tripoli is  $-11.3 \pm 9.4\%$ , though postwar  $\text{NO}_2$  levels (2013–2014) are similar to prewar levels (2005–2010). That is, the depression in  $\text{NO}_2$  levels in 2011 occurred in the latter half of the data record, causing the linear fit to show a decrease despite similar  $\text{NO}_2$  levels before and after the depression.

**Syria (unrest 2011 to present).** Civil unrest began in early 2011 in Syria and transitioned into civil war by the end of 2011. About 10.8 million of Syria's 22 million people are estimated to be in need of humanitarian assistance [United Nations High Commissioner for Refugees (UNHCR), 2015]. There are large decreases in  $\text{NO}_2$  levels over large areas of Syria (Figure 11), including the cities of Damascus ( $-37.1 \pm 10.9\%$ ) and Aleppo ( $-40.2 \pm 13.6\%$ ). The Battle of Aleppo has been ongoing since July 2012, which is consistent with the decrease in levels after 2011 (Figure 12). Though there has been less disruption in Damascus, the damage of the ongoing war (e.g., 6.5 million internally displaced persons within Syria [UNHCR, 2015]) on the Syrian economy and infrastructure [UNHCR, 2015] may have produced the decrease in  $\text{NO}_2$  levels over the city (Figure 12) as well as the entire country. There are no GDP data available for Syria after 2007 with which to assess the influence of the unrest on the country's economy [World Bank, 2015].

There are large increases in  $\text{NO}_2$  levels from 2005 to 2014 in all of the countries neighboring Syria, except Israel (Figure 11). The GDP's (constant 2005 U.S. dollar) of Lebanon, Turkey, and Jordan increased by 43%, 33%, and 41%, respectively, from 2005 to 2014 [World Bank, 2015]. However, Figure 12 shows that the changes in  $\text{NO}_2$  levels mainly occurred after the onset of the war in 2011, possibly indicating a causal effect.

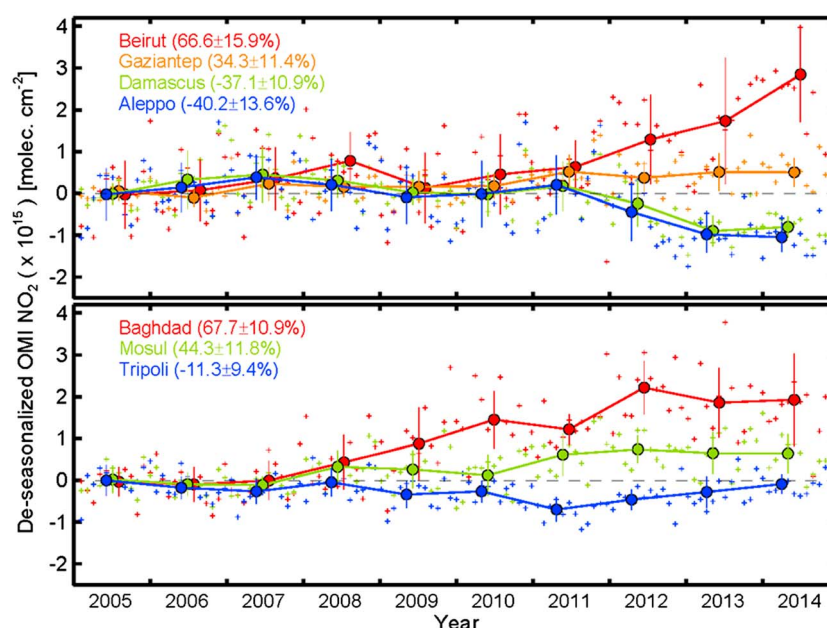


**Figure 12.** Deseasonalized (i.e., linear + residual terms) monthly OMI NO<sub>2</sub> data ( $\times 10^{15}$  mol/cm<sup>2</sup>) for several Middle Eastern cities. Monthly and annual average values are shown as pluses (+) and circles, respectively. The vertical bars on the annual average values represent the standard deviation for a given year.

There were large influxes of Syrian refugees into Lebanon (1.15 million), Jordan (625 thousand), and Turkey (1.6 million) from 2011 to 2014 [UNHCRb, 2015]. The Syrian refugee population in Lebanon accounts for ~20% of the country's prewar population and is stressing the country's limited infrastructure [UNHCRa, 2015]. The NO<sub>2</sub> increase in Beirut is  $66.6 \pm 15.9\%$  and NO<sub>2</sub> levels are elevated from 2012 to 2014 relative to the earlier period (Figure 12), which is also discussed by Lelieveld *et al.* [2015]. In Jordan, ~20% of Syrian refugees live in camps while the rest live in towns in the northern part of the country [UNHCRa, 2014]. About 30% of the Syrian refugees in Turkey are in camps and towns near the Turkish-Syrian border [UNHCRb, 2014], which is consistent with the location of the increases. For example, the NO<sub>2</sub> increase for Gaziantep (Turkey) is  $34.3 \pm 11.4\%$  (Figure 12).

*Iraq (unrest 2003 to present).* The Iraq War began with the U.S. invasion in 2003 and ended with official withdrawal at the end of 2011. However, civil conflict escalated after the U.S. withdrawal, including an insurgency by the Islamic State of Iraq and the Levant (ISIL or ISIS) that began in earnest in 2014. NO<sub>2</sub> levels increased over the whole of Iraq from 2005 to 2014 (Figure 11). The large increases near Mosul and Kirkuk are likely associated with oil extraction activities, as they are located in areas with substantial oil deposits, and oil production has increased despite the unrest [Organization of the Petroleum Exporting Countries (OPEC), 2015]. The increase in OMI NO<sub>2</sub> levels over Baghdad mostly occurred between 2009 and 2012 (Figure 12), which cannot be readily explained by variations in Iraq's GDP annual growth rate during this period [World Bank, 2015]. However, the Iraqi GDP annual growth does not give information on possible regional heterogeneity within the country. NO<sub>2</sub> levels in Baghdad peaked in 2012 and decreased slightly afterward, which is consistent with the escalation of civil conflict followed by the ISIL insurgency. During this period, there was a concomitant contraction of the Iraqi economy (i.e., the GDP annual growth rate was  $-6.4\%$  in 2014 but positive in all previous years [World Bank, 2015]), which may account for the depressed NO<sub>2</sub> levels.

The signatures of other conflicts around the world during the OMI record (2005–2014), such as those in Egypt and Nigeria, are not evident in the OMI NO<sub>2</sub> data. This may have occurred, as the scale of the conflict was small relative to the size of the economy so that NO<sub>x</sub> emissions were not significantly lower.

### 3.6. Cities in the Tropics and Subtropics

NO<sub>2</sub> levels in many cities in the tropics and subtropics of Latin America, Africa, South Asia (section 3.2), and Southeast Asia are lower than in more industrialized countries (Figure 1) and heavily influenced by the cycle



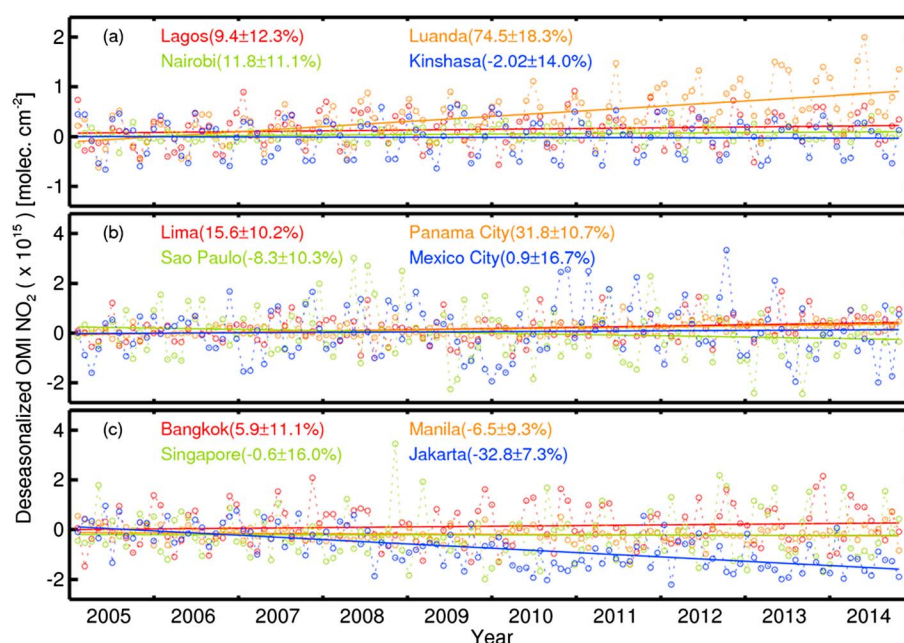


**Figure 13.** Deseasonalized (i.e., linear + residual terms) monthly OMI  $\text{NO}_2$  ( $\times 10^{15}$  mol/cm<sup>2</sup>) for various cities of the tropics and subtropics.

of the wet and dry seasons (e.g., Dhaka (Bangladesh; Figure 8); Lagos (Nigeria) and Bangkok (Thailand) in Figure S1). For example, Ghude *et al.* [2008], Prasad *et al.* [2012], and others find that  $\text{NO}_2$  levels in most areas of Pakistan, India, and Bangladesh are lowest during the wet season (June–September), as deep convection effectively ventilates the surface layer, and highest during the dry season (December–May). Seasonal biomass burning pollution that typically occurs at the end of the dry season, a month or two before the onset of the monsoonal rains [e.g., Duncan *et al.*, 2003], may amplify the annual  $\text{NO}_x$  cycle for many cities. Therefore, changes in  $\text{NO}_2$  levels for some cities may be influenced by year-to-year variations in seasonal burning.

**Africa.** There is a mix of changes in  $\text{NO}_2$  levels over African cities (Table S7 and Figure 13a). The largest increase ( $74.5 \pm 18.3\%$ ) is over Luanda, Angola's only major city, which has a metropolitan population of  $\sim 6.5$  million. The city's increase in  $\text{NO}_2$  levels is consistent with the country's strong population growth ( $\sim 38\%$  from 2005 to 2014) and economic development (i.e., 116% increase in GDP (constant 2005 U.S. dollar) from 2005 to 2014 [World Bank, 2015]), following the end of decades of civil war in 2002. The increase is clear in both the wet and dry seasons, unlike the majority of other world cities in our study that experience monsoons (Figure S1). Cities with decreases are Tripoli (Libya; section 3.5) and all major cities in South Africa (section 3.7). Increases occur over parts of South Africa (section 3.7) and the Nile River delta. Increases over the Sahel region may be related to changes in biomass burning.

**Latin America.** As with Africa, changes in  $\text{NO}_2$  levels over cities in Central and South America are mixed (Table S9 and Figure 13b). Notable increases (15–35%) occur in Lima (Peru), Salvador (Brazil), Panama City (Panama), and Santiago (Chile). The only significant decreases occur in a few cities in Mexico, such as Mazatlan and Guadalajara ( $\sim 15\text{--}20\%$ ). Mexico City displays considerable spatial heterogeneity, with large increases to the west and north of the city center and large decreases in the city center and to the northeast. Insignificant changes occur to the south. Over Latin America, there are no large regional changes (Figure S2), except over the Brazilian Amazon (e.g., the Brazilian states of Rondônia, Mato Grosso, and Pará) in areas which have undergone deforestation in the last few decades. This decrease in  $\text{NO}_2$  levels may occur as deforestation rates in 2013 are about a third of those in 2005, steadily declining through our study period [Nepstad *et al.*, 2014].

**Southeast Asia.** Most cities in this region have insignificant changes (Table S8 and Figures 13c and S4). The only significant increase occurs over Yangon (Myanmar). The decrease in Jakarta (Indonesia;  $-32.8 \pm 7.3\%$ ) is large and may be associated with emission controls put on vehicles beginning in 2005 [Nugroho *et al.*, 2005] and not



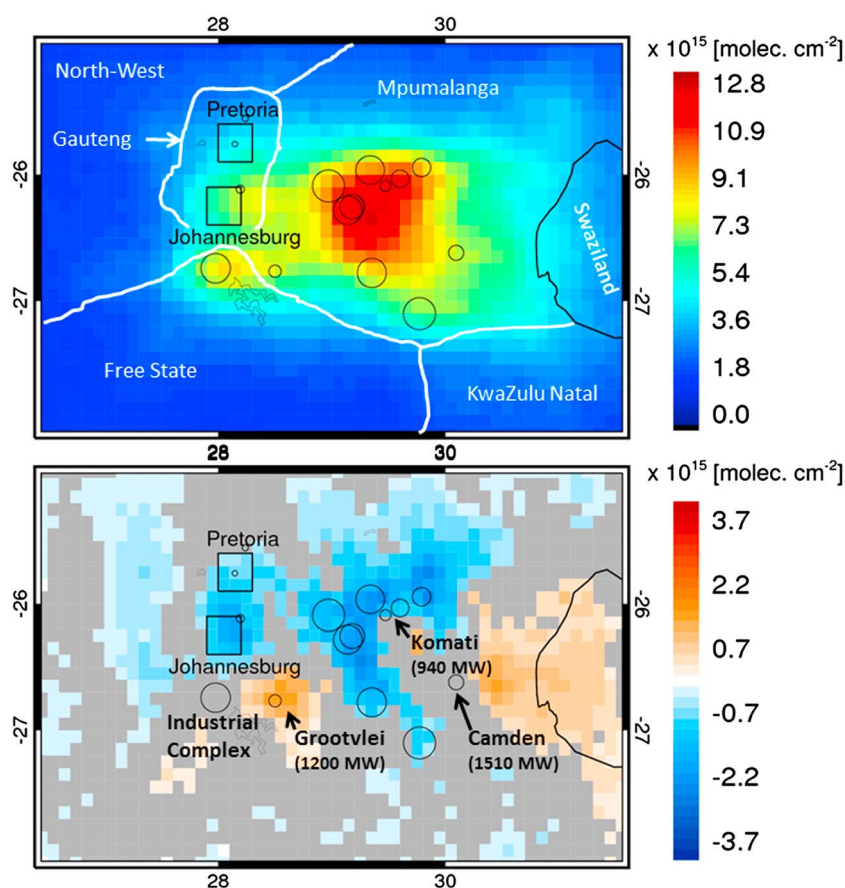


**Figure 14.** (top) OMI  $\text{NO}_2$  data ( $\times 10^{15}$  mol/ $\text{cm}^2$ ;  $0.1^\circ$  latitude  $\times 0.1^\circ$  longitude) as an annual average for 2014 over Johannesburg-Pretoria megacity (indicated by boxes) and surroundings. Thermal power plants are indicated by circles, where the size of the circle is proportional to electricity generation capacity. White lines indicate the approximate locations of provincial boundaries. (bottom) The absolute change of OMI  $\text{NO}_2$  data ( $\times 10^{15}$  mol/ $\text{cm}^2$ ) between 2005 and 2014. The named plants were shuttered in the early 1990s energy crises and returned to service by 2010. Gray areas represent where there are no statistically significant changes.

economic contraction as Indonesia's GDP (constant 2005 U.S. dollar) increased by 65% from 2005 to 2014 [World Bank, 2015]. The only area with moderate absolute increases occurs over northern Vietnam in the Red River Delta, which includes the industrial cities of Hanoi and Haiphong. The country's GDP (constant 2005 U.S. dollar) increased by 70% from 2005 to 2014 [World Bank, 2015].

### 3.7. A Case Study of a Complex Source Region: Johannesburg-Pretoria and Mpumalanga (South Africa)

The  $\text{NO}_2$  changes over Johannesburg, Cape Town, and Durban are  $-24.0 \pm 13.9\%$ ,  $-17.7 \pm 7.5\%$ , and  $-19.6 \pm 11.1\%$ , respectively (Table S7) from 2005 to 2014, while South Africa's GDP (constant 2005 U.S. dollar) increased by 28% over the same period [World Bank, 2015]. The decreases in  $\text{NO}_2$  are likely associated with the turnover of the fleet to more fuel-efficient vehicles, particularly in Cape Town and Durban which have light industry and no large thermal power plants. All new automobiles manufactured after 2008 are required to meet emission specifications in South Africa [United Nations Economic and Social Council (UNESCO), 2005]. While there is some spatial variability in the changes (predominantly decreases) around Cape Town and Durban (not shown), the region around the Johannesburg-Pretoria (J-P) conurbation shows both large decreases over Mpumalanga Province and large increases in two areas, one south of J-P and another to the east near the Swaziland border (Figure 14).

The J-P megacity and nearby Mpumalanga Province, an area of coal mining, thermal power generation, metal mining, and metallurgical industry [Jaars et al., 2014; USEIA, 2015d], contribute to a well-known satellite  $\text{NO}_2$  feature [e.g., Lourens et al., 2012] (Figure 14). Aircraft sampling over these regions, with multiaxis differential

optical absorption spectroscopy [Heue *et al.*, 2008], has confirmed the general features and west-east NO<sub>2</sub> gradient displayed by OMI (Figure 14). A recent study with surface data from five monitoring sites in the power plant region (circles in Mpumalanga Province, Figure 14) shows no significant NO<sub>2</sub> trend during the years 1990–2007 [Balashov *et al.*, 2014].

The OMI NO<sub>2</sub> changes in the J-P megacity and Mpumalanga Province represent a case study to illustrate the advantages of high-resolution data for interpreting changes in an area with a complex mixture of sources. The changes described below are generally consistent with data on thermal (essentially coal-fired) power generation that are regularly published for this region. However, comprehensive independent data for other NO<sub>x</sub> emissions in the overall region (e.g., mining, manufacturing, petrochemical industry, and biofuels use in small towns) are not available over the OMI period. For example, elevated NO<sub>2</sub> levels south of Johannesburg in southern Gauteng Province and northern Free State originate from intensive industry and some thermal power generation in the Vaal Triangle; this heavily polluted area is labeled “Industrial Complex” in Figure 14.

The exact causes of the large decreases (10–30%) over Mpumalanga Province are not known, although some association with NO<sub>x</sub> emissions by the eight large thermal power plants is suggested by the match of shape of the area of large decreases with the distribution of the facilities (Figure 14). The existing power plants did not employ emission control devices or change coal type during our study period. Eskom, South Africa’s primary energy supplier, plans the implementation of emission control devices within the next decade to meet new environmental regulations [Eskom, 2014]. South African electricity production increased by 27% from 2005 to 2014 with most of the increase occurring between 2005 and 2008 [Central Intelligence Agency (CIA), 2015], but coal consumption over this period varied only about  $\pm 5\%$  [USEIA, 2015d]. Total NO<sub>x</sub> emissions from all Eskom facilities increased by 13% from 2005 to 2007/2008 and by 7% from 2005 to 2014/2015 but decreased by 5% from 2007/2008 to 2014/2015. This possibly indicates that NO<sub>x</sub> emissions from the eight large thermal power plants decreased more than 5% from 2007/2008 to 2014/2015 since three shuttered facilities were returned to service. There were also likely variations in NO<sub>x</sub> emissions from colocated industrial activity, such as mining, metal work, and chemical production. For example, there were events such as a 5 month platinum miner’s strike in 2014 [Stoddard, 2014]; presumably, mining and metallurgical industry interruptions would have reduced NO<sub>x</sub> emissions and possibly reduced demands on electricity production.

The large NO<sub>2</sub> increases shown in Figure 14 may partially be associated with the reactivation of three shuttered thermal power plants beginning in 2008 to keep up with demand after a period of rolling blackouts (2007–2008) and starting again in 2014 [Financial Mail, 2015]. One of these is the reactivated Grootvlei facility which is located within a large area of increases, relatively isolated from other plants and with a clear signal. However, the reactivated Komati and Camden facilities are located in Mpumalanga Province so that any changes associated with their plumes are convolved with the changes of eight higher-emitting power-producing facilities and heavy industry that surround them. Nevertheless, NO<sub>x</sub> emissions from the relatively isolated Camden plant may be the source of the large area of increases east of the plant near Swaziland, as there are no thermal power plants or major industry of which we are aware in that area. The facility’s plume contributes more to the total NO<sub>2</sub> level when its plume is transported by westerly winds into an area of much lower NO<sub>2</sub> levels to the east than in other directions to areas with much higher NO<sub>2</sub> levels (Figure 14).

#### 4. Summary and Conclusions: A Critical Need for a High-Resolution Observing Strategy for Tropical and Subtropical Megacities

We present high-resolution changes in OMI NO<sub>2</sub> levels for many of the world’s largest cities and indicate the possible causes of these changes and their spatial structure. We discuss these changes in the context of potential drivers, such as (1) economic growth and associated energy consumption (e.g., South Asia), (2) compliance with local, regional, and/or country environmental regulations (e.g., U.S., Europe, and Japan), (3) possible regional pollution transport (e.g., the Republic of Korea and Japan), (4) civil unrest (e.g., Syria, Iraq, and Libya), and (5) efforts to deal with rapid urbanization and inadequate infrastructure (e.g., South Africa) and ambitious infrastructure development (e.g., India and the Republic of Korea).

We find evidence that the mixture of NO<sub>x</sub> sources within many of the world’s megacities has evolved significantly over the OMI record, 2005–2014. This evolution may persist in the coming decades as urbanization continues, economies grow/contract, environmental regulations are adopted and/or enforced, and

governments attempt to modernize infrastructure. For example, the Indian government has an ambitious plan, Ultra Mega Projects, to increase India's electricity generation capacity [Min. Power, 2015], many Indian cities are investing in infrastructure (e.g., commuter rail systems [Min. Urb. Develop, 2015]), and there are proposals for major industrial development (e.g., Delhi-Mumbai Industrial Corridor and Mumbai Urban Infrastructure Project; Min. Ind. Pol. and Prom., 2015). Chinese pollutant emissions may decrease as (1) the government amended its Environmental Protection Law in 2014 to strengthen its provision's enforcement and China's Premier "declared war" on pollution [e.g., Blanchard and Stanway, 2015] and (2) public demand for cleaner air has intensified over the last few years [e.g., Gardner, 2015].

High-resolution NO<sub>2</sub> data will likely be an important element of any observing strategy for inferring changes in energy consumption and coemitted pollutants and greenhouse gases that are not easily observed from spaceborne instruments. Currently, there are three geostationary satellites under development that will provide higher resolution NO<sub>2</sub> observations than OMI over portions of (1) East Asia (Geostationary Environment Monitoring Spectrometer), (2) North America (Tropospheric Emissions: Monitoring of Pollution), and (3) Europe (Sentinel-4), but these satellites will cover very few of the world's tropical and subtropical megacities. Though not geostationary, the upcoming TROPospheric Ozone Monitoring Instrument (TROPOMI), which is expected to launch in 2016, will provide higher spatial resolution data than OMI. While TROPOMI certainly holds promise for some pollutants, complementary surface observations will also be necessary to quantify pollutant and greenhouse gas emissions in complex source regions.

Looking forward, there is a critical need for an observational strategy that consists of coordinated orbital (i.e., satellite) and suborbital (i.e., surface networks and field campaigns) components to monitor air pollutant and greenhouse gas emissions in the world's tropical and subtropical megacities. Large increases in pollutant and greenhouse gas emissions are expected [e.g., Lioussé et al., 2014; Yan et al., 2014] as the world's population is expected to grow by 2.4 billion people by 2050, with most of that growth occurring in tropical and subtropical megacities [United Nations, 2013]. The development of an observational strategy for these regions is particularly important since most tropical and subtropical megacities lack surface observational networks.

## Acknowledgments

This work was supported by funding from the NASA Aura Mission and the NASA Applied Sciences Program. We thank Can Li (NASA) and Debra Wicks Kollonige (University of Maryland) for very helpful comments. The data are publicly available from the NASA Goddard Earth Sciences Data Active Archive Center (GES DISC; <http://disc.sci.gsfc.nasa.gov>).

## References

- Akimoto, H., Y. Mori, K. Sasaki, H. Nakanishi, T. Ohizumi, and Y. Itano (2015), Analysis of monitoring data of ground-level ozone in Japan for long-term trend during 1990–2010: Causes of temporal and spatial variation, *Atmos. Environ.*, **102**, 302–310, doi:10.1016/j.atmosenv.2014.12.001.
- Balashov, N. V., A. M. Thompson, S. J. Piketh, and K. E. Langerman (2014), Surface ozone variability and trends over the South African Highveld from 1990 to 2007, *J. Geophys. Res. Atmos.*, **119**, 4323–4342, doi:10.1002/2013JD020555.
- Blanchard, B., and D. Stanway (2015), "China to 'declare war' on pollution, premier says", Reuters News Agency. [Available at <http://www.reuters.com/article/2014/03/05/us-china-parliament-pollution-idUSBREA2405W20140305>.]
- Boersma, K. F., R. Braak, and R. J. van der A (2011), "Dutch OMI NO<sub>2</sub> (DOMINO) data product v2.0: HE5 data file user manual". [Available at [http://www.temis.nl/docs/OMI\\_NO2\\_HE5\\_2.0\\_2011.pdf](http://www.temis.nl/docs/OMI_NO2_HE5_2.0_2011.pdf).]
- Bowman, K. W. (2013), Toward the next generation of air quality monitoring: Ozone, *Atmos. Environ.*, **80**, 571–583, doi:10.1016/j.atmosenv.2013.07.007.
- Bucsela, E., N. Krotkov, E. Celarier, L. Lamsal, W. Swartz, P. Bhartia, K. Boersma, J. Veefkind, J. Gleason, and K. Pickering (2013), A new algorithm for retrieving vertical column NO<sub>2</sub> from nadir-viewing satellite instruments: Applications to OMI, *Atmos. Meas. Tech.*, **6**, 2607–2626, doi:10.5194/amt-6-2607-2013.
- Castellanos, P., and F. Boersma (2012), Reductions in nitrogen oxides over Europe driven by environmental policy and economic recession, *Sci. Rep.*, **265**, doi:10.1038/srep00265.
- Chan, C. K., and X. Yao (2008), Air pollution in mega cities in China, *Atmos. Environ.*, **42**, 1–42, doi:10.1016/j.atmosenv.2007.09.003.
- Chinese Assoc. of Auto. Manuf. (2014), Chinese Association of Automobile Manufacturers. [Available at <http://www.caam.org.cn/english/>.]
- CIA (2015), The World Factbook. [Available at <https://www.cia.gov/library/publications/resources/the-world-factbook/>.]
- Dickerson, R. R., M. O. Andreae, T. Campos, O. L. Mayol-Bracero, C. Neusuess, and D. G. Streets (2002), Analysis of black carbon and carbon monoxide observed over the Indian Ocean: Implications for emissions and photochemistry, *J. Geophys. Res.*, **107**(D19), 8017, doi:10.1029/2001JD000501.
- Dobber, M., R. Voors, R. Dirksen, Q. Kleipool, and P. Levelt (2008), The high-resolution solar reference spectrum between 250 and 550 nm and its application to measurements with the ozone monitoring instrument, *Solar Phys.*, **249**, 281–291, doi:10.1007/s11207-008-9187-7.
- Duncan, B., R. Martin, A. Staudt, R. Yevich, and J. Logan (2003), Interannual and seasonal variability of biomass burning emissions constrained by satellite observations, *J. Geophys. Res.*, **108**(D2), 4040, doi:10.1029/2002JD002378.
- Duncan, B., Y. Yoshida, B. de Foy, L. Lamsal, D. Streets, Z. Lu, K. Pickering, and N. Krotkov (2013), The observed response of Ozone Monitoring Instrument (OMI) NO<sub>2</sub> columns to NO<sub>x</sub> emission controls on power plants in the United States: 2005–2011, *Atmos. Environ.*, **81**, 102–111, doi:10.1016/j.atmosenv.2013.08.068.
- Duncan, B., et al. (2014), Satellite data of atmospheric pollution for U.S. air quality applications: Examples of applications, summary of data end-user resources, answers to FAQs, and common mistakes to avoid, *Atmos. Environ.*, **98**, 647–662, doi:10.1016/j.atmosenv.2014.05.061.
- Eskom (2014), 2014 Integrated Report. [Available at <http://integratedreport.eskom.co.za/pdf/full-integrated.pdf>.]
- Euro (2007), Regulation (EC) No 715/2007 of the European Parliament and of the Council of 20 June 2007 on type approval of motor vehicles with respect to emissions from light passenger and commercial vehicles (Euro 5 and Euro 6) and on access to vehicle repair and maintenance information 29.6.2007, Official Journal of the European Union L 171/1.

- Fang, M., C. K. Chan, and X. Yao (2009), Managing air quality in a rapidly developing nation: China, *Atmos. Environ.*, **43**, 79–83, doi:10.1016/j.atmosenv.2008.09.064.
- FEZ (2003), Free Economic Zones in Korea: The future of Northeast Asia, Planning Office of Free Economic Zone Ministry of Finance and Economy, Foreign Press and Public Relations Division, Ministry of Finance and Economy. [Available at <http://unpan1.un.org/intradoc/groups/public/documents/apcity/unpan018745.pdf>.]
- FEZ (2015), [Available at <http://www.fez.go.kr/en/incheon-fez-overview.jsp>.]
- Financial Mail (2015), "South Africa's energy crisis, 2008–2015", Financial Mail, Times Media Books. [Available at <http://cdn.bdlive.co.za/ebooks/Eskom%20and%20the%20SA%20energy%20crisis.pdf>.]
- Fishman, J., et al. (2008), Remote sensing of tropospheric pollution from space, *Bull. Am. Meteorol. Soc.*, **89**, 805–821, doi:10.1175/2008BAMS2526.1.
- Gardner, D. K. (2015), China's "Silent Spring" moment? Why "Under the Dome" found a ready audience in China, New York Times, 18 Mar. [Available at [http://www.nytimes.com/2015/03/19/opinion/why-under-the-dome-found-a-ready-audience-in-china.html?\\_r=0](http://www.nytimes.com/2015/03/19/opinion/why-under-the-dome-found-a-ready-audience-in-china.html?_r=0).]
- Ghude, S. D., S. Fadnavis, G. Beig, S. D. Polade, and R. J. van der A (2008), Detection of surface emission hot spots, trends, and seasonal cycle from satellite-retrieved NO<sub>2</sub> over India, *J. Geophys. Res.*, **113**, D20305, doi:10.1029/2007JD009615.
- Ghude, S. D., P. S. Kulkarni, S. H. Kulkarni, S. Fadnavis, and R. J. van der A (2011), Temporal variation of urban NO<sub>x</sub> concentration in India during the past decade as observed from space, *Int. J. Remote Sens.*, **32**, 3, doi:10.1098/01431161.2010.517797.
- Gu, D., Y. Wang, C. Smeltzer, and Z. Liu (2013), Reduction in NO<sub>x</sub> emission trends over China: Regional and seasonal variations, *Environ. Sci. Technol.*, **47**, 12,912–12,919, doi:10.1021/es401727e.
- Guttikunda, S. K., and P. Jawahar (2014), Atmospheric emissions and pollution from the coal-fired thermal power plants in India, *Atmos. Environ.*, **92**, 449–460, doi:10.1016/j.atmosenv.2014.04.057.
- Guttikunda, S. K., R. Goel, and P. Pant (2014), Nature of air pollution, emission sources, and management in the Indian cities, *Atmos. Environ.*, **95**, 501–510, doi:10.1016/j.atmosenv.2014.07.006.
- Heue, K.-P., T. Wagner, S. P. Broccardo, D. Walter, S. J. Piketh, K. E. Ross, S. Beirle, and U. Platt (2008), Direct observation of two dimensional trace gas distributions with an airborne Imaging DOAS instrument, *Atmos. Chem. Phys.*, **8**(22), 6707–6717, doi:10.5194/acp-8-6707-2008.
- Hilboll, A., A. Richter, and J. P. Burrows (2013), Long-term changes of tropospheric NO<sub>2</sub> over megacities derived from multiple satellite instruments, *Atmos. Chem. Phys.*, **13**, 4145–4169, doi:10.5194/acp-13-4145-2013.
- Hillger, D., et al. (2013), First-light imagery from suomi npp viirs, *Bull. Am. Meteorol. Soc.*, **94**, 1019–1029, doi:10.1175/BAMS-D-12-00097.1.
- Jaars, K., et al. (2014), Ambient aromatic hydrocarbon measurements at Welgegund, South Africa, *Atmos. Chem. Phys.*, **14**, 7075–7089, doi:10.5194/acp-14-7075-2014.
- Jacobson, M. Z., S. V. Nghiem, A. Sorichetta, and N. Whitney (2015), Ring of impact from the mega-urbanization of Beijing between 2000 and 2009, *J. Geophys. Res. Atmos.*, **120**, 5740–5756, doi:10.1002/2014JD023008.
- Jin, H. (2013), Korea's Incheon Airport embarks on \$4.6 bln expansion, Reuters, 26 Sept. [Available at <http://www.reuters.com/article/2013/09/26/incheon-airport-idUSL4N0HK0ZE20130926>.]
- Jin, X., and T. Holloway (2015), Spatial and temporal variability of ozone sensitivity over China observed from the Ozone Monitoring Instrument, *J. Geophys. Res. Atmos.*, **120**, 7229–7246, doi:10.1002/2015JD023250.
- Kim, S.-W., A. Heckel, S. A. McKeen, G. J. Frost, E.-Y. Hsie, M. K. Trainer, A. Richter, J. P. Burrows, S. E. Peckham, and G. A. Grell (2006), Satellite-observed U.S. power plant NO<sub>x</sub> emission reductions and their impact on air quality, *Geophys. Res. Lett.*, **33**, L22812, doi:10.1029/2006GL027749.
- Krotkov, N., et al. (2015), Aura OMI observations of regional SO<sub>2</sub> and NO<sub>2</sub> pollution changes from 2005 to 2014, *Atmos. Chem. Phys. Discuss.*, **15**, 26,555–26,607, doi:10.5194/acpd-15-26555-2015.
- Kurokawa, J., T. Ohara, T. Morikawa, S. Hanayama, G. Janssens-Maenhout, T. Fukui, K. Kawashima, and H. Akimoto (2013), Emissions of air pollutants and greenhouse gases over Asian regions during 2000–2008: Regional Emission inventory in ASia (REAS) version 2, *Atmos. Chem. Phys.*, **13**, 11,019–11,058, doi:10.5194/acp-13-11019-2013.
- Lamsal, L. N., R. V. Martin, D. D. Parrish, and N. A. Krotkov (2013), Scaling relationship for NO<sub>2</sub> pollution and urban population size: A satellite perspective, *Environ. Sci. Technol.*, **47**(14), 7855–7861, doi:10.1021/es400744g.
- Lamsal, L. N., et al. (2014), Evaluation of OMI operational standard NO<sub>2</sub> column retrievals using in situ and surface-based NO<sub>2</sub> observations, *Atmos. Chem. Phys.*, **14**, 11,587–11,609, doi:10.5194/acp-14-11587-2014.
- Lamsal, L. N., B. N. Duncan, Y. Yoshida, N. A. Krotkov, K. E. Pickering, D. G. Streets, and Z. Lu (2015), U.S. NO<sub>2</sub> trends (2005–2013): EPA Air Quality System (AQS) data versus improved observations from the Ozone Monitoring Instrument (OMI), *Atmos. Environ.*, **110**, 130–143, doi:10.1016/j.atmosenv.2015.03.055.
- Lee, H.-J., S.-W. Kim, J. Brioude, O. R. Cooper, G. J. Frost, C.-H. Kim, R. J. Park, M. Trainer, and J.-H. Woo (2014), Transport of NO<sub>x</sub> in East Asia identified by satellite and in situ measurements and Lagrangian particle dispersion model simulations, *J. Geophys. Res. Atmos.*, **119**, 2574–2596, doi:10.1002/2013JD021185.
- Lee, J.-W., and K. Hong (2012), Economic growth in East Asia: Determinants and prospects, *Jpn. World Econ.*, **24**, 101–113, doi:10.1016/j.japwor.2012.01.005.
- Lei, Y., Q. Zhang, K. B. He, and D. G. Streets (2011), Primary anthropogenic aerosol emission trends for China, 1990–2005, *Atmos. Chem. Phys.*, **11**, 931–954, doi:10.5194/acp-11-931-2011.
- Lelieveld, J., S. Beirle, C. Hörmann, G. Stenchikov, and T. Wagner (2015), Abrupt recent trend changes in atmospheric nitrogen dioxide over the Middle East, *Sci. Adv.*, **1**(7), e1500498, doi:10.1126/sciadv.1500498.
- Li, C., Q. Zhang, N. A. Krotkov, D. G. Streets, K. He, S.-C. Tsay, and J. F. Gleason (2010), Recent large reduction in sulfur dioxide emissions from Chinese power plants observed by the Ozone Monitoring Instrument, *Geophys. Res. Lett.*, **37**, L08807, doi:10.1029/2010GL042594.
- Li, R., and G. Leung (2012), Coal consumption and economic growth in China, *Energy Policy*, **40**, 438–443, doi:10.1016/j.enpol.2011.10.034.
- Lin, J.-T., D. Pan, and R.-X. Zhang (2013), Trend and interannual variability of Chinese air pollution since 2000 in association with economic development: A brief overview, *Atmos. Oceanic Sci. Lett.*, **6**(2), 84–89, doi:10.1080/16742834.2013.11447061.
- Liousse, C., E. Assamoi, P. Crique, C. Granier, and R. Rosset (2014), Explosive growth in African combustion emissions from 2005 to 2030, *Environ. Res. Lett.*, **9**, 035003, doi:10.1088/1748-9326/9/3/035003.
- Liu, F., Q. Zhang, D. Tong, B. Zheng, M. Li, H. Huo, and K. B. He (2015a), High-resolution inventory of technologies, activities, and emissions of coal-fired power plants in China from 1990 to 2010, *Atmos. Chem. Phys. Discuss.*, **15**, 13,299–13,317, doi:10.5194/acpd-15-18787-2015.
- Liu, Z., et al. (2015b), Reduced carbon emission estimates from fossil fuel combustion and cement production in China, *Nature*, **524**, 335–338, doi:10.1038/nature14677.



- Lourens, A. S., T. Butler, J. Beukes, P. G. van Zyl, B. Steffen, T. Wagner, K.-P. Heue, J. J. Pienaar, G. Fourier, and M. Lawrence (2012), Re-evaluating the NO<sub>2</sub> hotspot over the South African Highveld, *S. Afr. J. Sci.*, **108**, 1146, doi:10.4102/sajs.v108i11/12.1146.
- Lu, Z., and D. G. Streets (2012), Increase in NO<sub>x</sub> Emissions from Indian thermal power plants during 1996–2010: Unit-based inventories and multisatellite observations, *Environ. Sci. Technol.*, **46**(14), 7463–7470, doi:10.1021/es300831w.
- Lu, Z., D. G. Streets, Q. Zhang, S. Wang, G. R. Carmichael, Y. F. Cheng, C. Wei, M. Chin, T. Diehl, and Q. Tan (2010), Sulfur dioxide emissions in China and sulfur trends in East Asia since 2000, *Atmos. Chem. Phys.*, **10**, 6311–6331, doi:10.5194/acp-10-6311-2010.
- Lu, Z., Q. Zhang, and D. G. Streets (2011), Sulfur dioxide and primary carbonaceous aerosol emissions in China and India, 1996–2010, *Atmos. Chem. Phys.*, **11**, 9839–9864, doi:10.5194/acp-11-9839-2011.
- McFarlane, S. (2009), *Air Quality Regulations and Odour Management in Australia and New Zealand*, 78 pp., Clean Air Society of Australia and New Zealand, Olinda, Vic. Aust.
- Min. Coal (2014), Provisional Coal Statistics 2013–14, Ministry of Coal, Government of India, p. 82. [Available at [http://coal.nic.in/sites/upload\\_files/coal/files/coalupload/provisional1314\\_0.pdf](http://coal.nic.in/sites/upload_files/coal/files/coalupload/provisional1314_0.pdf).]
- Min. Environ (2015), 2014 Environmental Statistics Yearbook, p. 710. [Available at <http://eng.me.go.kr/eng/web/index.do>.]
- Min. Ind. Pol. and Prom (2015), Annual Report 2014–15, Ministry of Industrial Policy and Promotion, Government of India, p. 248. [Available at [http://dipp.nic.in/English/Publications/Annual\\_Reports/AnnualReport\\_Eng\\_2014-15.pdf](http://dipp.nic.in/English/Publications/Annual_Reports/AnnualReport_Eng_2014-15.pdf).]
- Min. Petrol. and Natural Gas (2015), Annual Report 2014–15, Ministry of Petroleum and Natural Gas, Government of India, p. 172. [Available at [http://petroleum.nic.in/docs/Annual\\_Report/AR14-15.pdf](http://petroleum.nic.in/docs/Annual_Report/AR14-15.pdf).]
- Min. Power (2015), Annual Report 2014–15, Ministry of Power, Government of India, p. 252. [Available at [http://powermin.nic.in/upload/pdf/Annual\\_Report\\_2014-15\\_English.pdf](http://powermin.nic.in/upload/pdf/Annual_Report_2014-15_English.pdf).]
- Min. Urb. Develop (2015), Annual Report 2014–15, Ministry of Urban Development, Government of India, p. 311. [Available at [http://moud.gov.in/sites/upload\\_files/moud/files/English%20Annual%20Report.pdf](http://moud.gov.in/sites/upload_files/moud/files/English%20Annual%20Report.pdf).]
- Mohammadi, H., D. Cohen, M. Babazadeh, and L. Rokni (2012), The effects of atmospheric processes on Tehran smog forming, *Iran J. Public Health*, **41**(5), 1–12.
- Nepstad, D., et al. (2014), Slowing Amazon deforestation through public policy and interventions in beef and soy supply chains, *Science*, **344**(6188), 1118–1123, doi:10.1126/science.1248525.
- Nugroho, S. B., A. Fujiwara, and J. Zhang (2005), Evaluating the effects of a new vehicle emission standard on urban air quality in Jakarta City, *J. Int. Dev. Coop.*, **11**(2), 11–30.
- OPEC (2015), Organization of the Petroleum Exporting Countries (OPEC) Monthly Oil Market Report, Editor: O. S. Abdul-Hamid, 13 July. [Available at [http://www.opec.org/opec\\_web/static\\_files\\_project/media/downloads/publications/MOMR\\_July\\_2015.pdf](http://www.opec.org/opec_web/static_files_project/media/downloads/publications/MOMR_July_2015.pdf).]
- Prasad, A. K., R. P. Singh, and M. Kafatos (2012), Influence of coal-based thermal power plants on the spatial-temporal variability of tropospheric NO<sub>2</sub> column over India, *Environ. Monit. Assess.*, **184**, 1891–1907, doi:10.1007/s10661-011-2087-6.
- PRDAIR (2014), Guangdong-Hong Kong-Macao Pearl River Delta Regional Air Quality Monitoring Network: A report of monitoring results in 2014, Report Number: PRDAIR-2014-5. [Available at [http://www.epd.gov.hk/epd/sites/default/files/epd/english/resources\\_publications/files/PRD\\_2014\\_report\\_en.pdf](http://www.epd.gov.hk/epd/sites/default/files/epd/english/resources_publications/files/PRD_2014_report_en.pdf).]
- Ramachandran, A., N. K. Jain, S. A. Sharma, and J. Pallipad (2013), Recent trends in tropospheric NO<sub>2</sub> over India observed by SCIAMACHY: Identification of hot spots, *Atmos. Poll. Res.*, **4**, 354–361, doi:10.5094/APR.2013.040.
- Randel, W. J., and J. B. Cobb (1994), Coherent variations of monthly mean total ozone and lower stratospheric temperature, *J. Geophys. Res.*, **99**, 5433–5447, doi:10.1029/93JD03454.
- Richter, A., J. P. Burrows, H. Nüß, C. Granier, and U. Niemeier (2005), Increase in tropospheric nitrogen dioxide over China observed from space, *Nature*, **437**, 129–132, doi:10.1038/nature04092.
- Russell, A. R., A. E. Perring, L. C. Valin, E. J. Bucsela, E. C. Browne, K.-E. Min, P. J. Wooldridge, and R. C. Cohen (2011), A high spatial retrieval of NO<sub>2</sub> column densities from OMI: method and evaluation, *Atmos. Chem. Phys.*, **11**, 8543–8554, doi:10.5194/acp-11-8543-2011.
- Russell, A. R., L. C. Valin, and R. C. Cohen (2012), Trends in OMI NO<sub>2</sub> observations over the United States: Effects of emission control technology and the economic recession, *Atmos. Chem. Phys.*, **12**(24), 12,197–12,209.
- Schneider, P., and R. J. van der A (2012), A global single-sensor analysis of 2002–2011 tropospheric nitrogen dioxide trends observed from space, *J. Geophys. Res.*, **117**, D16309, doi:10.1029/2012JD017571.
- Schneider, P., W. Lahoz, and R. van der A (2015), Recent satellite-based trends of tropospheric nitrogen dioxide over large urban agglomerations worldwide, *Atmos. Chem. Phys.*, **15**, 1205–1220, doi:10.5194/acp-15-1205-2015.
- SEB (2012), Shanghai Environmental Bulletin. [Available at [http://www.sepb.gov.cn/fa/cms/shhj/file/2013bulletin/en/eh\\_0001.html](http://www.sepb.gov.cn/fa/cms/shhj/file/2013bulletin/en/eh_0001.html).]
- Shin, H., K. Cho, J. Han, J. Kim, and Y. Kim (2012), The effects of precursor emission and background concentration changes on the surface ozone concentration over Korea, *Aerosol Air Qual.*, **12**, 93–103, doi:10.4209/aaqr.2011.09.0141.
- Stoddard, E. (2014), South Africa miners return to work after longest platinum strike, Reuters, 25 June. [Available at <http://www.reuters.com/article/2014/06/25/us-safrica-mining-idUSKBN0F00DC20140625>.]
- Streets, D., et al. (2013), Emissions estimation from satellite retrievals: A review of current capability, *Atmos. Environ.*, **77**, 1011–1042, doi:10.1016/j.atmosenv.2013.05.051.
- Takashima, H., H. Irie, Y. Kanaya, and H. Akimoto (2011), Enhanced NO<sub>2</sub> at Okinawa Island, Japan caused by rapid air-mass transport from China as observed by MAX-DOAS, *Atmos. Environ.*, **45**(15), 2593–2597, doi:10.1016/j.atmosenv.2010.10.055.
- Technology, A. (2015), Incheon International Airport (ICA/RKSI), South Korea. [Available at <http://www.airport-technology.com/projects/incheon-international-airport/>.]
- Tong, D., L. Lamsal, L. Pan, C. Ding, H. Kim, P. Lee, T. Chai, K. E. Pickering, and I. Stajner (2015), Long-term NO<sub>x</sub> trends over large cities in the United States during the great recession: Comparison of satellite retrievals, ground observations, and emission inventories, *Atmos. Environ.*, **107**, 70–84, doi:10.1016/j.atmosenv.2015.01.035.
- Total (2015). [Available at <http://www.total.com/en/energies-expertise/oil-gas/refining-petrochemicals/projects-achievements/total-invests-upgrade-daesan-south-korea?FFbw=kludge1%FF>.]
- ul-Haq, Z., S. Tariq, M. Ali, K. Mahmood, S. A. Batool, and A. D. Rana (2014), A study of tropospheric NO<sub>2</sub> variability over Pakistan using OMI data, *Atmos. Pollut. Res.*, **5**, 709–720, doi:10.5094/APR.2014.080.
- UNESC (2005), United Nations Economic and Social Council, Distr. GENERAL TRANS/WP.29/GRPE/50, Informal document No. GRPE-50-20 (50th GRPE, 30 May–3 June 2005, agenda item 8.), Republic of South Africa: Recently Gazetted and imminent vehicle emission legislation: GRPE June 2005.
- UNHCRa (2014), UNHR Global Appeal Update, Jordan, United Nations High Commissioner for Refugees. [Available at <http://www.unhcr.org/5461e6070.html>.]
- UNHCRa (2015), UNHR Global Appeal Update, Syrian Arab Republic, United Nations High Commissioner for Refugees. [Available at <http://www.unhcr.org/5461e60716.html>.]

- UNHCRb (2014), UNHR Global Appeal Update, Turkey, United Nations High Commissioner for Refugees. [Available at <http://www.unhcr.org/5461e60c52.html>.]
- UNHCRb (2015), UNHR global trends, forced displacement in 2014, United Nations High Commissioner for Refugees, 18 June. [Available at <http://www.unhcr.org/556725e69.html>.]
- United Nations (2013). [Available at <https://www.un.org/en/development/desa/news/population/un-report-world-population-projected-to-reach-9-6-billion-by-2050.html>.]
- USBLS (2012), BLS spotlight on statistics, The Recession of 2007–2009. [Available at [http://www.bls.gov/spotlight/2012/recession/pdf/recession\\_bls\\_spotlight.pdf](http://www.bls.gov/spotlight/2012/recession/pdf/recession_bls_spotlight.pdf).]
- USEIA (2013), U.S. Energy Information Administration, 12 July. [Available at <http://www.eia.gov/todayinenergy/detail.cfm?id=12071>.]
- USEIA (2015a), U.S. Energy Information Administration "Independent Statistics & Analysis, Drilling Productivity Report", 13 July. [Available at <http://www.eia.gov/petroleum/drilling/pdf/dpr-full.pdf>.]
- USEIA (2015b), India, International energy data and analysis, U.S. Energy Information Administration, p. 23. [Available at [http://www.eia.gov/beta/international/analysis\\_includes/countries\\_long/India/india.pdf](http://www.eia.gov/beta/international/analysis_includes/countries_long/India/india.pdf).]
- USEIA (2015c), China, International energy data and analysis, U.S. Energy Information Administration, p. 36. [Available at [http://www.eia.gov/beta/international/analysis\\_includes/countries\\_long/China/china.pdf](http://www.eia.gov/beta/international/analysis_includes/countries_long/China/china.pdf).]
- USEIA (2015d), South Africa, International energy data and analysis, U.S. Energy Information Administration, p. 11. [Available at [http://www.eia.gov/beta/international/analysis\\_includes/countries\\_long/South\\_Africa/south\\_africa.pdf](http://www.eia.gov/beta/international/analysis_includes/countries_long/South_Africa/south_africa.pdf).]
- Wakamatsu, S., T. Morikawa, and A. Ito (2013), Air pollution trends in Japan between 1970 and 2012 and impact of urban air pollution countermeasures, *Asian J. Atmos. Environ.*, 7–4, 177–190, doi:10.5572/ajae.2013.7.4.177.
- Wang, S., D. G. Streets, Q. Zhang, K. He, D. Chen, S. Kang, Z. Lu, and Y. Wang (2010), Satellite detection and model verification of NO<sub>x</sub> emissions from power plants in Northern China, *Environ. Res. Lett.*, 5, 044007, doi:10.1088/1748-9326/5/4/044007.
- Wang, S. W., Q. Zhang, D. G. Streets, K. B. He, R. V. Martin, L. N. Lamsal, D. Chen, Y. Lei, and Z. Lu (2012), Growth in NO<sub>x</sub> emissions from power plants in China: Bottom-up estimates and satellite observations, *Atmos. Chem. Phys.*, 12, 4429–4447, doi:10.5194/acp-12-4429-2012.
- Wang, S. X., et al. (2014), Emission trends and mitigation options for air pollutants in East Asia, *Atmos. Chem. Phys.*, 14, 6571–6603, doi:10.5194/acp-14-6571-2014.
- WHO (2014), Ambient (outdoor) air pollution in cities database 2014. [Available at [http://www.who.int/phe/health\\_topics/outdoorair/databases/cities/en/](http://www.who.int/phe/health_topics/outdoorair/databases/cities/en/).]
- Witte, J., B. Duncan, A. Douglass, T. Kurosu, K. Chance, and C. Retscher (2011), The unique OMI HCHO/NO<sub>2</sub> feature during the 2008 Beijing Summer Olympics: Implications for ozone production sensitivity, *Atmos. Environ.*, 45, 3103–3111, doi:10.1016/j.atmosenv.2011.03.015.
- World Bank (2015), World Data Bank of the World Bank. [Available at <http://databank.worldbank.org/data/>.]
- World Dev. Ind (2015), World Development Indicators, The World Bank. [Available at <http://data.worldbank.org/data-catalog/world-development-indicators>.]
- Yan, F., E. Winijkul, D. G. Streets, Z. Lu, T. C. Bond, and Y. Zhang (2014), Global emission projections for the transportation sector using dynamic technology modeling, *Atmos. Chem. Phys.*, 14, 5709–5733, doi:10.5194/acp-14-5709-2014.
- Yue, M. (2014), Joint effort to fight Delta pollution, Shanghai Daily Newspaper, 8 Jan. [Available at <http://www.shanghaidaily.com/Metro/environment/Joint-effort-to-fight-Delta-pollution/shdaily.shtml>.]
- Zhang, Q., et al. (2007), NO<sub>x</sub> emission trends for China, 1995–2004: The view from the ground and the view from space, *J. Geophys. Res.*, 112, D22306, doi:10.1029/2007JD008684.
- Zhang, Q., D. G. Streets, and K. He (2009), Satellite observations of recent power plant construction in Inner Mongolia, China, *Geophys. Res. Lett.*, 36, L15809, doi:10.1029/2009GL038984.
- Zhong, L., P. K. K. Louie, J. Zheng, K. M. Wai, J. W. K. Ho, Z. Yuan, A. K. H. Lau, D. Yue, and Y. Zhou (2013), The Pearl River Delta Regional Air Quality Monitoring Network—Regional Collaborative Efforts on Joint Air Quality Management, *Aerosol Air Qual. Res.*, 13, 1582–1597, doi:10.4209/aaqr.2012.10.0276.
- Zhou, Y., D. Brunner, C. Hueglin, S. Henne, and J. Staehelin (2012), Changes in OMI tropospheric NO<sub>2</sub> columns over Europe from 2004 to 2009 and the influence of meteorological variability, *Atmos. Environ.*, 46, 482–495, doi:10.1016/j.atmosenv.2011.09.024.